FINAL REPORT

DEVELOPMENT OF AN ELECTROMAGNETIC INDUCTION FLOWMETER FOR CRYOGENIC FLUIDS

Prepared for National Aeronautics and Space Administration

Under Contract No. NASw — 381

EPCO ENGINEERING-PHYSICS COMPANY

5615 RANDOLPH ROAD • ROCKVILLE • MARYLAND

ENGINEERING-PHYSICS COMPANY
5515 Randolph Road
Rockville, Maryland

Final Report

DEVELOPMENT OF AN ELECTROMAGNETIC INDUCTION FLOWMETER FOR CRYOGENIC FLUIDS

By Vincent Cushing, Dean Reily, and George Edmunds
EPCO Project No. 105

Prepared for Lewis Research Center
National Aeronautics and Space Administration

Under Contract No. NASw-381

15 May 1964

FORWARD

In December of 1960 under contract NASr-13 the staff of the Engineering-Physics Company carried out a study concerning the feasibility of an electromagnetic flowmeter for use with dielectric fluids, including the cryogenic propellants. Thereafter, under contract NASr-53, an experimental investigation was completed by December of 1961; the results showed clearly that the electromagnetic flowmeter was indeed operable with dielectric fluids such as transformer oil. With these very encouraging and fruitful theoretical and experimental results in hand, EPCO thereupon--under the subject contract NASw-381--designed, developed, and tested a vacuum-jacketed model designed to measure flowrates of liquid hydrogen (LH_2) up to 1 pound/second.

The problems encountered and solved in the work which we now report have been mostly of a mechanical design nature. One major problem has been the development of a dielectric (fiberglas) transducer tube with attendant liner and end seals which is workable (i.e., maintains a good seal so that the insulating vacuum may be maintained on the outside of the tube while its interior is filled with pressurized LH_2) with the more conventional stainless steel plumbing found in LH_2 flow systems. A second major problem has been the development of triaxial electrical connectors which maintain a vacuum-tight seal on the one hand and at the same time maintain electrically noise-free contact with the temperature shocked transducer tube on the other. The solution to these problems has permitted the electromagnetic flowmeter to produce the excellent experimental data described in Section V of this report.

From the electromagnetic point of view, the design of the flowmeter described in this report is basically the same as that evolved during the engineering analysis and experimental verification phases which preceded the work reported herein.

The authors would like to express their gratitude to Mr. I. Warshawsky of the Instrument Research Laboratory of NASA's Lewis Research Center for the valuable technical advice he has given since the beginning of this overall effort in 1960.

Respectfully submitted,

ENGINEERING-PHYSICS COMPANY

Vincent J. Cushing

Dean M. Reily

George W. Edmunds

TABLE OF CONTENTS

CONTENTS Concluded

LIST OF ILLUSTRATIONS

ILLUSTRATIONS Concluded

DEVELOPMENT OF AN ELECTROMAGNETIC INDUCTION FLOWMETER FOR CRYOGENIC FLUIDS

Final Report

I. INTRODUCTION

This is the final report under contract NASw-381, which has been concerned with the development of an electromagnetic (EM) induction flowmeter for use with liquid hydrogen (LH_2). The work reported herein was commenced in December 1961 and concluded in September 1963. Preliminary research and development had been carried out by the Engineering-Physics Company for the National Aeronautics and Space Administration under contracts NASr-13 and NASr-53.

The electromagnetic induction flowmeter for dielectric fluids--originally conceived by the staff of the Engineering-Physics Company late in 1960 and proposed as a research and development program to the National Aeronautics and Space Administration in that same year--has reached a stage of development where experimental results have been excellent and are in complete agreement with the theoretical model which has been concomitantly evolved. New plumbing practice problems, peculiar to the use of LH_2 with the induction flowmeter's dielectric transducer tube, have been solved; and it has been established that a flow signal is obtainable even with the quite stringent electrical characteristics of liquid hydrogen. The device currently is operable when temperature equilibrium is reached in the transducer tube.

The electromagnetic induction flowmeter[1,2] has long been hoped for[3] as an ideal device for application to jet engines and rockets. That the electromagnetic induction flowmeter is excellent for jet engine and rocket applications becomes understandable if one simply enumerates its physical and operating characteristics:

1. Obstructionless--no pressure drop;
2. No moving parts;
3. Linearity over extreme dynamic range--including flow in either direction;
4. Extreme sensitivity to flow variation or flow oscillation*;
5. Volumetric flow measurement which is insensitive to the fluid's electrical properties or variations thereof; and in the same instrument, by an alternate setting of a switch;
6. Massmetric measurement for non-polar fluids (regardless of phase) such as the cryogenic propellants;
7. Self-calibration capability in the field.

---

[1]Vincent Cushing, Rev. Sci. Instr., 29,692 (1958); 32, 225 (1961).

[2]J. A. Shercliff, The Theory of Electromagnetic Flow Measurement, Cambridge University Press, 1962.

[3]A. H. Blessing and H. Menes, "Report of Acceptance Test of the Magneflow Electromagnetic Flowmeter," Technical Note No. 30, U. S. Naval Air Rocket Test Station, Lake Denmark, Dover, New Jersey, August 6, 1953.

*And the flowmeter's rapid responding output voltage can be smoothed or filtered if smooth flow totalization is desired.

Sufficient conditions for the proper operation of the electromagnetic flowmeter are: (1) the flow velocity profile be symmetric with respect to the axis of the flowmeter; (2) the electrical properties of the metered fluid be macroscopically uniform throughout the sensing section of the electromagnetic flowmeter. For a two-phase fluid in the massmetric mode, the latter condition implies that such a mixture must be something like a foam; however, the quality of the foam may vary between zero and one. Whether and to what degree of accuracy the electromagnetic flowmeter will operate with stratified two-phase mixtures is a subject which requires more research. Meanwhile, if highly stratified two-phase flow is a matter of serious importance, the user of the EM flowmeter should establish some kind of an homogenizer (e.g., a turbulence screen) upstream of the flow sensing section.

The electromagnetic flowmeter has a long history of successful operation in the laboratory and has an eight year history of success in industrial applications. However, prior to the very recent research and development effort conducted at the Engineering-Physics Company, the electromagnetic flowmeter had been thought workable only when used with liquids of sufficiently large electrical conductivity. The earlier, inadequate theoretical understanding of the electromagnetic flowmeter was the underlying cause of repeated and consistent failure in an extensive series of projects, extending from 1949 to 1960--by private industry as well as by contractors to NACA, the Air Force, and the Navy--to develop a flowmeter workable with low conductivity and dielectric liquids such as JP4 and RP1. With this long standing, clearcut

history of failure there had never been any suggestion or hope of employing an electromagnetic flowmeter with the extremely dielectric cryogenic propellants.

Based on more recent theoretical considerations[4], EPCO proposed almost three years ago to investigate experimentally a new technique for making the electromagnetic flowmeter workable with dielectric fluids, including liquid hydrogen. In the ensuing investigation electromagnetic flowmeters have been designed, constructed and operated successfully with transformer oil, liquid nitrogen, and liquid hydrogen. Theory and experiment have evolved so that today all experimental facts are in quantitative agreement with the theoretical model--a model which is expressed in terms of all component and design parameters (e.g., capacities, dimensions, etc.).

In Section II of this report we describe the theory of operation of the electromagnetic flowmeter, and indicate how it works in both the volumetric as well as the massmetric mode. In Section III we describe the electronic and mechanical configuration of the existing flowmeter; and in Section IV we carry out an error analysis which describes the accuracy attainable with this flowmeter in terms of the various component tolerances. Section V describes the test and operating procedures, and also gives the results of test runs in a liquid hydrogen test facility. The specific details of the mechanical and electrical design are provided in the several Appendices to this report.

---

[4] Vincent Cushing, loc. cit.

II. THEORY OF OPERATION

In this Section we should like to describe the electrical equivalent circuit for the electromagnetic flowmeter, and in terms of this to describe quantitatively the flowmeter voltage output for both volumetric and massmetric flow measurement. See Section III for a schematic of the physical configuration of the electromagnetic flowmeter.

A. Equivalent Circuit

Fig. 1 is the electrical equivalent circuit of the electromagnetic flowmeter. The important parameters may be discussed as follows:

V_F -- The flow-induced voltage in volts, which is directly proportional to the volumetric flowrate through the flowmeter. We shall see in this Section how this flow voltage can be simply modified to provide rigorously a voltage which is proportional to massrate of flow for all non-polar fluids (in the liquid or vapor state) such as H_2,O_2, F_2, N_2, etc. It has been shown[5] that

$$V_F = \frac{BF}{a} \frac{\sin \beta}{E(\beta,1)} \quad , \quad (1)$$

where B is the (rms) magnetic induction in webers per square meter;

F is the volumetric flowrate in cubic meters per second;

β is the semi-angle subtended by the curvilinear detection electrode;

$E(\beta,1)$ is a tabulated[6] elliptic integral;

a is the interior radius of the transducer tube.

---

[5] Vincent Cushing and Dean Reily, "Induction Flowmeter for Dielectric Fluids --Engineering Analysis," Final Report to NASA under Contract NASr-13, March 22, 1961, p. 40.

[6] Jahnke-Emde-Losch, Tables of Higher Functions, 6th Edition, McGraw-Hill Book Company, New York, 1960, p. 43 ff.

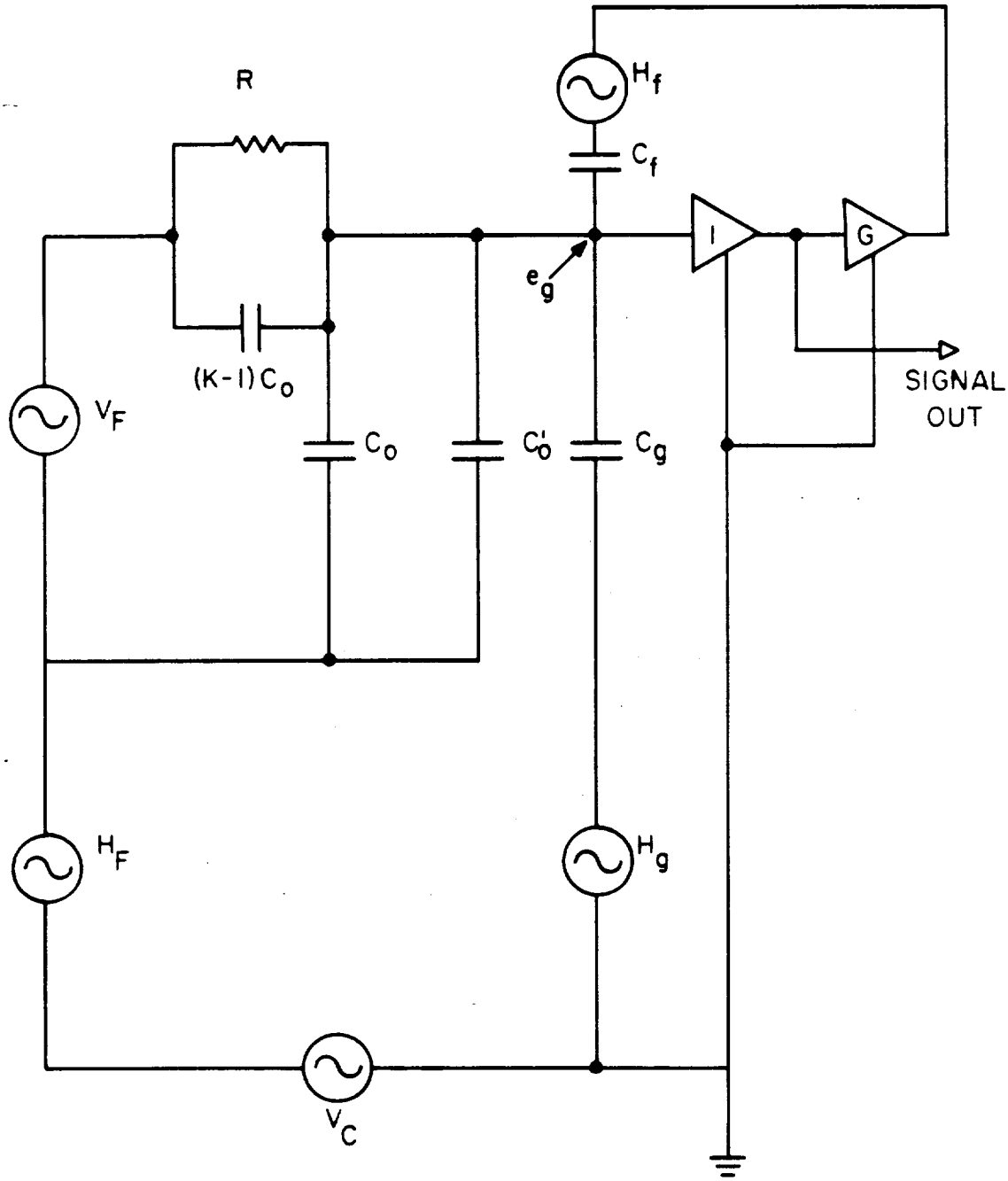

Fig. 1 Equivalent circuit of the electromagnetic induction flowmeter.

C_o -- The vacuum internal capacitance between the detection electrode and the compensation electrode. For our flowmeter configuration this has been shown[7] to be

$$C_o = \frac{2LK_o}{\pi} E(\beta,1) \quad , (2)$$

where L is the length (parallel to the axis of the transducer tube) of the detection and compensation electrodes, in meters;

K_o is the permittivity of free space, 8.85 picofarads per meter.

K -- The dielectric constant of the metered fluid, dimensionless.

R -- The resistance through the transducer tube between the detection electrode and compensation electrode. By consideration of the electrical relaxation time of the dielectric fluid, this may readily be shown to be, for our flowmeter configuration

$$R = K_o/\sigma C_o = \frac{\pi}{2\sigma L\ E(\beta,1)} \quad , (3)$$

where σ is the electrical conductivity of the metered fluid in mhos per meter.

C_o' -- Is the fringe capacity between the detection electrode and the compensation electrode. Ideally, one should have all of the electrical lines of flux between the detection and compensation electrodes pass through the metered fluid; however, in the electromagnetic induction flowmeter we do know that some of the electrical lines of flux between the detection and compensation electrodes fringe around the fiberglas transducer tube. Since the dielectric

---

[7] Vincent Cushing and Dean Reily, loc. cit. p. 43.

constant of the fiberglas tube varies considerably with temperature, this fringe capacitance may be expected to contribute some measure of temperature sensitivity to the existing flowmeter.

C_g -- The residual capacitance to ground from the detection electrode. The driven-shield electrode is designed to minimize the capacitance to ground, but nonetheless a residual capacitance to ground does exist. By measurement, the value of C_g is the order of one or two picofarads, which is comparable to the internal capacitance C_o of the flowmeter. Again, the lines of electric flux between the detection electrode and ground pass through fiberglas and they also fringe to some extent through the metered fluid; hence, we can expect that this residual capacitance to ground is a contributor to the present flowmeter's temperature sensitivity.

C_f -- The direct capacitance between the driven-shield electrode and the detection electrode. In the present LH_2 electromagnetic flowmeter the magnitude of this capacitance has been measured to be approximately 45 picofarads. As shown in Fig. 1, regenerative feedback from the amplifier is fed through this feedback capacitance C_f. As we shall note in Eq. (4) below, the calibration constant of our flowmeter depends quite sensitively on the value of C_f. If we now recall that all of the electric lines of flux between the driven-shield electrode and the detection electrode pass through fiberglas, and recall that the dielectric constant of fiberglas will decrease appreciably in colling-down to cryogenic temperatures, it is evident that the calibration constant of our flowmeter will not become stable until temperature equilibrium has been obtained. Since the theemal diffusivity of fiberglas is not large, a considerable amount of time is required for this

temperature equilibrium to obtain. Hence the LH_2 electromagnetic flowmeter is not yet suited for measurement during the thermal shock attendant to the start-up of a cryogenic flow system.

H_F

H_g -- Hum generators due to imperfect symmetry. These hum generators are essentially due to the "transformer effect"[8]. Since the circuitry leading to each of the essential electrodes in the flow transducer passes through a strong, alternating magnetic induction, it is to be generally expected that a "transformer effect" EMF will be generated. It is well known that such "transformer effect" hums are in time quadrature with the magnetic induction (i.e., they are proportional to $\partial B/\partial t$), whereas the flow-induced signal, as seen by Eq. (1), is in-phase with the magnetic induction. By mechanical design symmetry one endeavors to make these hum generators equal to zero; but because of practicable fabrication tolerances, one may expect some residual hum even so. In order to discriminate against any residual hum the present LH_2 flowmeter makes use of a phase-sensitive detector which rejects such hum (a quadrature voltage) and provides a dc output which is in direct proportion to the flow-generated voltage. If, because of fabrication tolerances, the net hum voltage should be more than, say, 30-50 times larger than the flow-generated voltage, there is danger that the amplifiers will become partially saturated so as to cause a slight phase shift in the signal; and then the phase-sensitive detector will begin to respond to hum voltages. In order to reduce any such excess hum voltage in the present

H_f

---

[8] Vincent Cushing, loc. cit.

LH_2 electromagnetic flowmeter we essentially inject a compensation voltage V_C as indicated in Fig. 1, of such magnitude and phase as to null the hum voltage due to the "transformer effect".

V_C -- The compensation voltage as described above. The source for this compensation voltage is the same reference loop, described in Section III, which also serves to provide the reference voltage for the phase-sensitive detector. This reference voltage is attenuated and, if necessary, slightly phase-shifted so as to effect a null of any residual hum voltage.

G -- The gain in the amplifier which is to be fed back regeneratively through the feedback capacitor C_f. In the electromagnetic induction flowmeter this regenerative feedback is effected between the driven-shield and detection electrodes within the transducer tube itself.

e_g -- The voltage at the grid of the input amplifier.

B. Fundamental Equation for Electromagnetic Induction Flowmeter

As indicated in the equivalent circuit of Fig. 1, the signal output is the same as the voltage e_g at the grid of the input to the amplifier. For simplicity henceforth we will neglect the metered fluid's resistance R since for the cryogenic propellants R [see Eq. (3)] is so large that it is entirely negligible in its effect upon the equivalent circuit in Fig. 1*. Neglecting the resistor R, then, we

---

*Furthermore, if the reader carries through an analysis including the equivalent resistor R he will find that the important facets are unchanged:

a. A gain setting G can be established such that the flow generated signal is independent of the electrical properties K and σ of the metered fluid;

b. The method of ascertaining the proper gain setting G by emptying the pipe of fluid as described below remains unchanged.

find from straightforward circuit analysis

$$e_g = \frac{(K-1)C_o V_F + (KC_o + C_o')(H_F + V_C) + C_g H_g + C_f H_f}{KC_o + C_o' + C_g + (1-G)C_f} \quad . \quad (4)$$

In connection with Eq. (4) we note that G is the gain which is regeneratively fed back through the capacitor C_f. The value of G is at our disposal--it is a design parameter.

C. Volumetric Mode of Operation

If we wish a flow signal e_g which is precisely equal to the volumetric flow-generated voltage V_F we must establish the gain G in Eq. (4) such that the coefficient of V_F is unity; that is, we must fix G such that

$$KC_o + C_o' + C_g + (1 - G_v)C_f = (K-1)C_o \quad , \quad (5)$$

or establish

$$G_v = 1 + \frac{C_o + C_o' + C_g}{C_f} \quad . \quad (6)$$

At first sight, Eq. (6) indicates the most valuable result that the gain setting G does not depend on the dielectric constant K of the fluid*. However, to the extent that C_o' and C_g have part of their electric flux lines fringing into the fluid, then to that extent C_o' and C_g are dependent on the dielectric constant K. In the electromagnetic induction flowmeter the dependence of these residual and fringe capacities on K is extremely slight so that little difficulty is encountered in this respect.

We must further recall in connection with the electromagnetic induction flowmeter that the capacities C_o', C_g, and very extensively C_f, depend on the dielec-

---

*And if we had carried through the resistor R in Fig. 1 we would have obtained Eq. (6) as written.

tric constant of the transducer tube; and since this dielectric constant changes appreciably with temperature cool-down to cryogenic temperatures we see that the induction flowmeter has a requirement for regenerative gain which depends on the temperature--or put another way, the present LH_2 flowmeter does not operate satisfactorily until temperature equilibrium is established. Further effort should be carried out to eliminate or adequately minimize this thermal transient problem.

If we now substitute Eq. (6) or Eq. (5) into Eq. (4) we obtain

$$e_g = V_F + \frac{(K + C_o'K_o)(H_F + V_C) + C_gH_g/C_o + C_fH_f/C_o}{K - 1} \quad . (7)$$

Eq. (7) demonstrates that we have our objective of having a measured voltage e_g which is equal to the flow-generated voltage V_F. We also see that the various hum voltages and the compensation voltage depend on the dielectric constant of the fluid. However, all of these voltages are in time quadrature with the flow signal, so that such voltages are rejected by the phase-sensitive detector, and a fortiori any changes in these voltages are rejected by the phase-sensitive detector.

D. <u>In-the-Field Test Procedure for Volumetric Mode of Operation</u>

In order to determine when the gain setting G is proper in accord with Eq. (6), we do the following. First we shut off the magnet so that the hum voltages as well as the flow-generated voltage [see Eq. (1)] are zero. Eq. (4) then reads

$$e_g/V_C = \frac{KC_o + C_o'}{KC_o + C_o' + C_g + (1 - G)C_f} \quad . (8)$$

If the gain setting G is established at the proper value indicated by Eq. (6) or by Eq. (5), then Eq. (8) becomes

$$e_g/V_C = \frac{K + C_o'/C_o}{K - 1} \quad . (9)$$

Eq. (9) indicates that with the transducer tube empty--so that K = 1--the gain G should be adjusted until the ratio e_g/V_C becomes very, very large--in practice just reaches the point of oscillation*. Thus we see that the proper gain setting for G can be established by injecting a standard voltage V_C into the compensation electrode of the flowmeter, then making adjustments on G until the output voltage e_g is at the point of oscillation. Thus we are afforced in the induction flowmeter a means of checking--in the field--to see whether the gain setting G is properly established to provide volumetric flow measurement regardless of the electrical properties of the fluid.

E. Massmetric Mode of Operation

To effect massflowrate measurement with this LH_2 electromagnetic flowmeter we resort to the Clausius-Mosotti equation[9], which is valid for fluids (whether liquid or gas) made up of non-polar molecules.

$$\rho M = (K - 1)/(K + 2) \quad , (10)$$

where ρ is the density of the fluid;

M is the Clausius-Mosotti constant proper to the constituent molecules in the fluid;

K is the bulk dielectric constant of the fluid.

Table I indicates the Clausius-Mosotti constant for the cryogenic propellant fluids of interest. [A molecule is non-polar (i.e., it has no permanent dipole moment) provided there is symmetry in the distribution of electrical charge in the molecule.]

---

*Because of the temperature sensitivity of the capacitance, C_o', the gain, G, has been set with liquid hydrogen in the transducer tube.

[9]Wolfgang K. H. Panofsky and Melba Phillips, Classical Electricity and Magnetism. Addison and Wesley Publishing Company, Reading, Mass., 1955, p. 33.

TABLE I

CLAUSIUS-MOSOTTI CONSTANTS

FOR CRYOGENIC FLUIDS

Fluid	Temperature (°K)	Density (g/cc)	Clausius-Mosotti Constant, M (cc/g)
LH_2	16	0.0752	0.9880[a]
	18	0.0732	0.9885[a]
	20	0.0712	0.9888[a]
LOX	55 and above		0.1211 ± 0.05%[b]
LF_2	85	1.11	0.113[c]
LN_2	68	0.854	0.1557[a]
	74	0.825	0.1556[a]

[a] Computed from density and dielectric data available in Russell B. Scott, Cryogenic Engineering, Van Nostrand, New York, 1959.

[b] Victor J. Johnson (General Editor), A Compendium of the Properties of Materials at Low Temperature (Phase I), Part 1: Properties of Fluids; WADD Tech. Rept. 60-56; conducted by National Bureau of Standards Cryogenic Engineering Laboratory, July, 1960, p. 7.005.

[c] Ibid. Dielectric constant data for fluorine is extremely sparse, and permitted computation (from knowledge of corresponding density) only at 85° K.

It is perhaps obvious that all homonuclear diatomic molecules--such as H_2, O_2, F_2, N_2. etc.--do have the symmetry such that there can be no permanent dipole moment; and indeed, theoretical as well as experimental determination of the dipole moment of such molecules bear this out. We shall see that this places tremendous value in the electromagnetic flowmeter in that it permits the flowmeter to operate, if desired, as a massflowmeter for the most interesting cryogenic propellants.

Depending on the symmetry of the molecule, other more complicated molecules may have the required symmetry and thus be non-polar. For example, the entire methane series--methane (CH_4), ethane (C_2H_6), propane (C_3H_8), butane (C_4H_{10}), etc. --among petroleum products is non-polar. Indeed, from cursory examination, it appears that a petroleum fluid such as RP1 is essentially made up of non-polar constituents. If, in such a heterogeneous fluid, the percent by weight of the several constituents is known to be (adequately) constant, then one can apply the Clausius-Mosotti theory, derive or measure the effective Clausius-Mosotti constant, and thereafter employ the electromagnetic flowmeter as a massflowmeter for such fluids as well.

To see how we employ the electromagnetic flowmeter to measure massflowrate of non-polar fluids we solve Eq. (10) for (K - 1), and substitute into our fundamental electromagnetic flowmeter equation, Eq. (4), to obtain

$$e_g = \frac{(K + 2)C_o DF_m + (KC_o + C_o')(H_F + V_C) + C_g H_g + C_f H_f}{KC_o + C_o' + C_g + (1 - G)C_f} \quad , \quad (11)$$

where the massflowrate F_m is defined by

$$F_m \equiv \rho F \quad , \quad (12a)$$

and D is a constant [see Eq. (1)] given by

$$D = \frac{BM}{a} \frac{\sin \beta}{E(\beta, 1)} \quad . \quad (12b)$$

Following our earlier line of reasoning, we should like to set the coefficient of DF_m equal to unity so that our measured flow voltage e_g will be linearly proportional to the massflowrate; and with constant of proportionality equal to D, as given in Eq. (12b). Thus, we must find a new gain setting G for our amplifier such that

$$KC_o + C_o' + C_g + (1 - G)C_f = (K + 2)C_o \quad , \quad (13)$$

or

$$G_m = 1 + \frac{C_o' + C_g - 2C_o}{C_f} \quad . \quad (14)$$

It is perhaps interesting to note that the difference in gain setting G for volumetric flow measurement and for massmetric flow measurement is expressed by

$$\Delta G \equiv G_v - G_m = 3C_o/C_f \quad . \quad (15)$$

We again have the result in Eq. (14) that the gain setting G_m for massmetric measurement is established only in terms of the physical constants of the flowmeter, and does not at all depend on the electrical properties of the fluid.

When the proper gain setting G_m is established, Eq. (11) reads

$$e_g = DF_m + \frac{(K + C_o'/C_o)(H_F + V_C) + C_g H_g/C_o + C_f H_f/C_o}{K + 2} \quad . \quad (16)$$

We see that there is a unique gain setting G_m which makes the electromagnetic flowmeter workable as a massflowmeter for all non-polar fluids. To be sure, an adjustment must be made to the final readout equipment (but not to the transducer amplifier) in order to have the proper scale setting corresponding to the value of D for the fluid being metered. Thus, a different readout scale setting must be used for massrate indication of LH_2, LOX, or LF_2.

F. In-the-Field Test Procedure for the Massmetric Mode of Operation

To determine the proper gain setting G_m we follow our earlier procedure: shut off the magnetic field and inject a standard voltage, V_C; Eq. (16) then becomes

$$e_g/V_C = \frac{K + C_o'/C_o}{K + 2} \quad . \quad (17)$$

Eq. (17) indicates that, if we know the dielectric constant K of the fluid in the transducer tube, then we must adjust G_m so that the gain e_g/V_C is as required by Eq. (17). Perhaps the medium with the most accurately known dielectric constant corresponds to an empty tube for which K = 1*. Under such conditions Eq. (17) reads

$$e_g/V_C = \frac{1 + C_o'/C_o}{3} \quad . \quad (18)$$

Hence, if in the electromagnetic induction flowmeter we know the magnitude of the fringe capacitance C_o' and the direct capacitance C_o between the detection electrode and the compensation electrode, we are able to adjust G_m until Eq. (18) is satisfied. When this gain setting G_m has been fixed, then the electromagnetic flowmeter functions as a massflowmeter for all non-polar fluids such as LH_2, LOX, and LF_2.

*Because of the temperature sensitivity of the capacitance, C_o', the gain, G, has been set with liquid hydrogen in the transducer tube.

III. ELECTRICAL AND MECHANICAL CONFIGURATION

The following two subsections contain a description of the electrical and mechanical configuration of the LH_2 electromagnetic flowmeter. Those readers desiring a more detailed description of the electrical and mechanical design are referred to the Appendices.

A. Electrical Configuration

The essential features of the electromagnetic flowmeter have been described in Section II of this report. In this subsection we will discuss in more detail the electronics used in the detection circuit and those used to provide the 10 kc power to drive the magnet coil.

The detection circuit used in the electromagnetic flowmeter has four functions:

1. Signal impedance transformation;
2. Flowmeter calibration;
3. Hum compensation;
4. Phase-sensitive detection.

Fig. 2 shows the basic flowmeter mechanical and electrical configuration. The electrical configuration is shown in more detail in the block diagram of Fig. 3. It should be noted that the four above-listed functions can be effected by the following controls on the control cabinet.

1. Run-Off-Calibration (Cal) switch;
2. The normal (Norm)-compensation (Comp) switch;
3. Compensation amplitude and phase control;
4. Signal amplitude and phase control.

While measuring flowrate the switches are in the RUN and NORM positions respectively.

The source impedance of the electromagnetic flowmeter is principally the reactance of a capacitance of the order of one picofarad; therefore, an impedance transformation is essential before transmitting the signal to the control cabinet. A preamplifier circuit with two pentode stages is mounted on the flowmeter housing and its input is connected to the detection electrode. Near unity degenerative feedback is employed in the preamplifier resulting in a highly stabilized amplifier with a voltage gain slightly greater than unity. The output signal of the preamplifier is then transmitted via cable to the control cabinet where its phase and amplitude may be controlled manually by a parallel resonant circuit having a variable capacitor for the control of the phase and a potentiometer to control the amplitude. A second two-stage pentode amplifier very similar to the preamplifier and having a voltage gain of near unity is then used to obtain another impedance transformation before transmission via cable of the signal back to the flowmeter. The return signal is used to drive the driven-shield electrode of the transducer tube. The phase of the return signal is normally made to coincide with the phase of the signal of the detection electrode by adjusting the phase control to compensate for any small phase shifts effected during the amplification of the signal.

Driving the driven shield at slightly greater than unity gain is tantamount to regenerative feedback so that the input of the preamplifier as seen by the transducer tube appears to have a negative input capacitance.

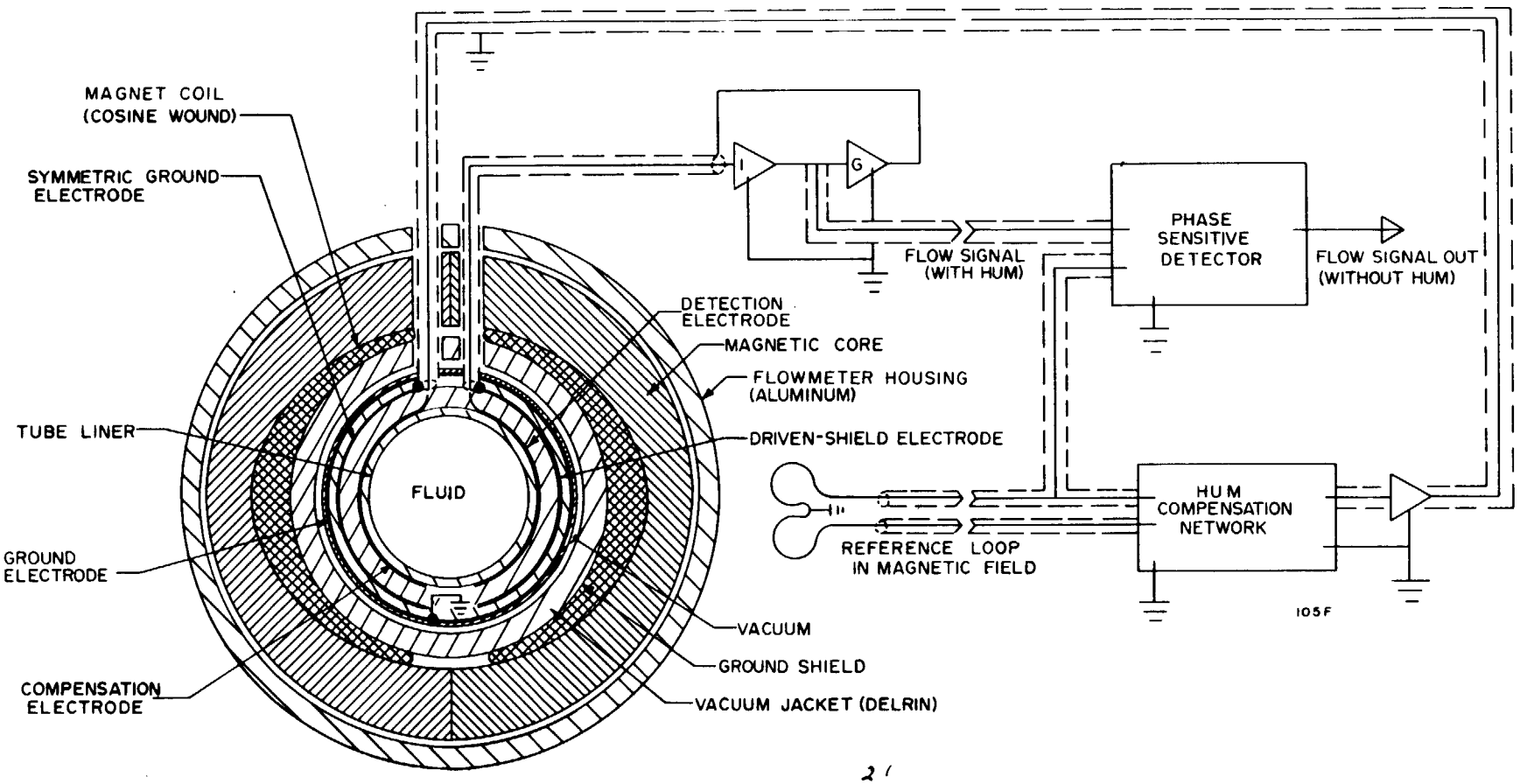

21

Fig. 2 Schematic of the liquid hydrogen electromagnetic induction flowmeter showing the flowmeter construction and the amplifier, phase-sensitive detector, and hum compensation network.

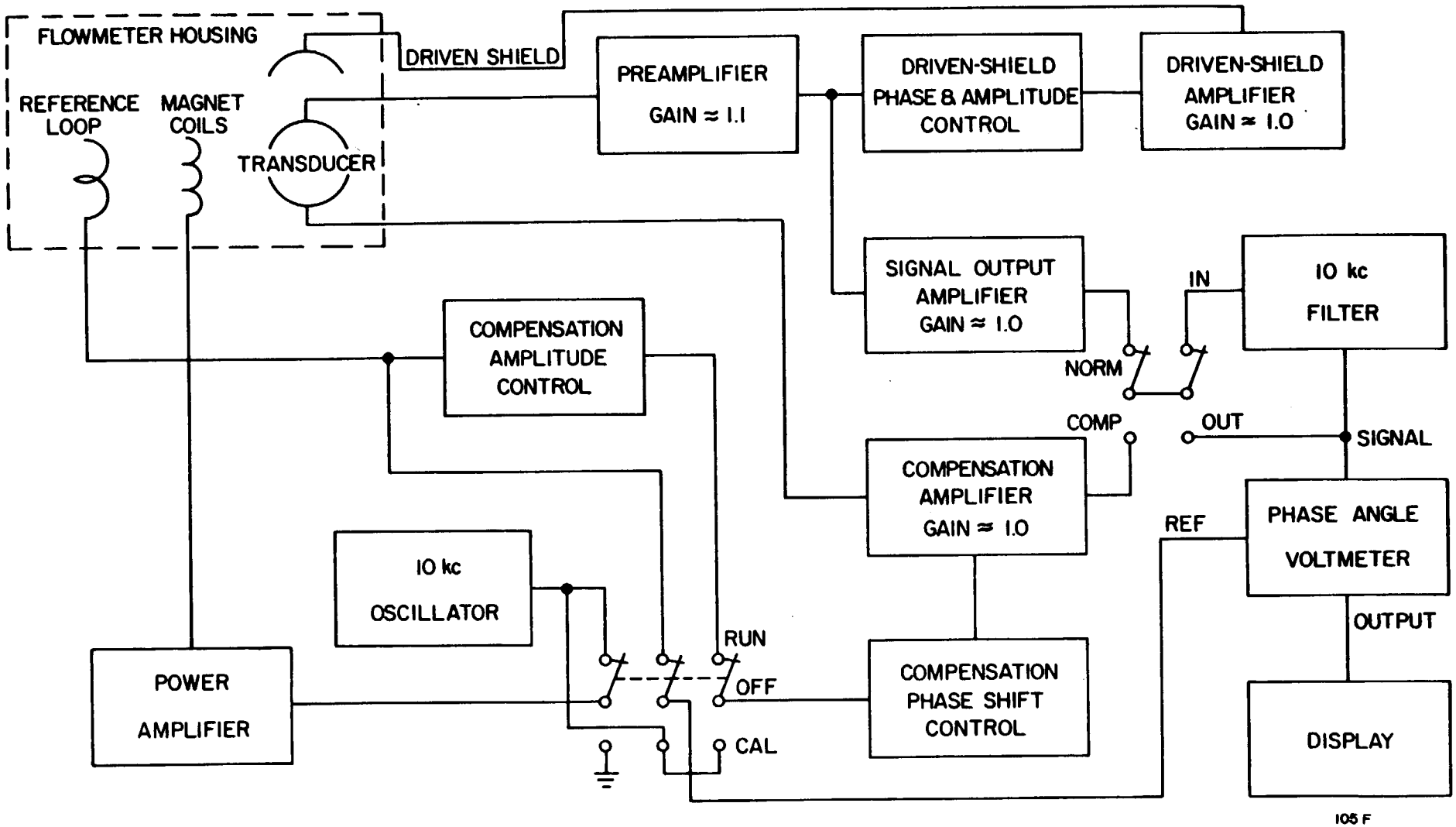

Fig. 3 Block diagram of flowmeter electrical configuration.

Using the amplitude control this negative capacitance can be so adjusted as to balance the positive transducer tube capacitance and hence results in the detection of a flow signal independent of the dielectric properties of the fluid. A detailed discussion of such operation is given in Section II.

We have now concluded our discussion of the impedance transformation technique and have nearly described the calibration technique. What remains is to show the way in which the regenerative gain is adjusted to attain the desired negative capacitance value. This is done by connecting the 10 kc oscillator, having known phase and amplitude, to the compensation electrode of the transducer tube. (Actually, a compensation amplifier is used as a buffer before transmission of the signal to the transducer tube.) The regenerative gain can then be fixed by means of the phase and amplitude control. The proper gain setting is discussed in Section II.

The origin and character of the "transformer effect" voltage or hum voltage have been described in Section II. While these hum voltages are in quadrature with the signal voltage they are of considerable amplitude relative to the signal voltage and must be reduced prior to amplification so as to avoid saturation of the amplifiers. Compensation of the hum voltage is accomplished by injecting a voltage on the compensation electrode which is equal to the hum voltage but opposite in phase. The compensation voltage is obtained from the reference loop (a copper wire loop magnetically coupled to the 10-kc alternating magnetic field developed by the magnet coil) and transmitted by cable to the control cabinet. The compensation voltage is then adjusted in phase and amplitude by the compensation controls and fed into the compensation

amplifier to attain an impedance transformation before transmission to the compensation electrode of the transducer tube.

Ideally, the compensation voltage could be made to completely compensate for the hum voltage; however, since in the present flowmeter the hum voltages are quite large, large compensation voltages are required. Hence, slight drift in either compensation or hum voltage can result in a voltage of significant amplitude relative to that of the flow signal.

In that some small remnant of hum voltage may be present after compensation and since it is in quadrature with the flow signal, phase sensitive detection is employed. In the present system a phase-angle voltmeter is used which consists essentially of signal channel and reference channel amplifiers, a set of lowpass filters for each of the channels, and a ring demodulator. The instrument can be adjusted for sensitivity to only those signals in a slected phase with respect to the voltage from the reference loop. In flowmeter operation the reference voltage is applied to the reference channel and the phase-angle voltmeter is set to detect the flow signal which is in quadrature with the reference voltage. A more detailed account of the actual circuits and circuit schematics is shown in Appendix F.

From the discussion of Section II the importance of the uniform alternating magnetic field of constant amplitude is evident since the flow signal sensed by the transducer tube is proportional to the (rms) intensity magnetic field as well as to the fluid flowrate. The magnet circuit consists simply of a series-connected pair of cosine wound coils oriented as shown in Fig. 2. These coils are parallel tuned to a resonant frequency of 10 kc and

driven by a power amplifier with input connected to a 10 kc crystal stabilized oscillator. The field strength can be adjusted by the gain control of the amplifier. A description of the magnet coils and magnet power supply is given in more detail in Appendix E.

B. Mechanical Configuration

Fig. 2 is a schematic of the essential features of the LH_2 electromagnetic flowmeter. The cross section of the magnet coil varies as a cosine function to establish a uniform magnetic induction in the transducer tube. The magnetic core which is placed around the outside of the magnet coil is used to minimize the reluctance of the overall magnetic circuit so that the magnetic induction will be as large as possible for a given current in the magnet windings.

The magnet coil and its magnetic core are supported on the outside diameter of a plastic cylinder which also serves as the outside jacket of an annular vacuum chamber. The inside wall of the vacuum chamber is formed by the transducer tube-liner combination. This vacuum area serves to insulate thermally the transducer tube from the rest of the flowmeter. The vacuum chamber is arranged coaxially with the transducer tube and connects at each end to a vacuum jacketed fluid line.

The transducer tube (see Fig. 2) contains the signal electrode, the compensation electrode, the driven-shield electrode, the symmetric ground electrode, and the ground electrode. These electrodes are fine grids of parallel conductors embedded in the tube, which is fabricated of fiberglas. A grid-type electrode was selected to eliminate eddy currents which would occur in a solid sheet conductor; the resultant counter mmf would attenuate the magnetic

field. The transducer tube also serves as the pressure container for use with a high pressure LH_2 flow system.

The transducer tube in the electromagnetic flowmeter must consist of a non-conducting section of dielectric pipe in order that it may be permeable to the 10 kc alternating magnetic induction. Fiberglas serves excellently for the transducer tube at LH_2 temperatures, and it has the added virtue of a quite high Young's modulus and very small shrinkage during cool-down. However, fiberglas is somewhat permeable to hydrogen--at least to an extent which makes it difficult to maintain adequate vacuum in the vacuum insulation--and so a Kel-F liner is used. The liner is flared at the ends to completely seal the transducer tube from the fluid.

Electrical leads from the transducer tube are brought out through the vacuum insulation in a sealed triaxial configuration. These leads connect the electronics to the detection electrode, the compensation electrode, and the driven-shield electrode. The ground electrode surrounding the other electrodes in the transducer tube is connected to the flowmeter housing through a grounding screw and lug.

The electronics or preamplifier section is enclosed with a removable cover which seals this section and permits the electronics section and magnetic coil to be pressurized with two atmospheres of an inert gas such as helium.

The various components and the overall mechanical design are discussed in considerable more detail in the Appendices. Appendix A describes the mechanical design features for the complete flowmeter and the construction

of the Delrin vacuum jacket. Appendix B describes the transducer tube design and fabrication techniques. Appendix C describes the development of the sealed triaxial (triax) connectors which connect the transducer tube to the flowmeter electronics. Appendix D discusses the development of a nonmetallic liner for containing cryogenic fluids.

IV. ERROR ANALYSIS

In this Section of the report we should like to provide an analytical expression which describes the error in the flowmeter's output voltage expressed as a function of the tolerances or errors in the several components which make up the flowmeter.

A. Volumetric Mode

To carry out an error analysis on the cryogenic electromagnetic flowmeter in its volumetric mode, we simply take the logarithmic derivative of Eq. (4). But before doing so we should note that there are certain auxiliary equations. The nominal value of the overall gain G is as described by Eq. (6); and when the hum voltages are nulled by the compensation voltage V_C, we have the following nominal equation [see Eq. (7)]

$$(K + C_o'K_o)(H_F + V_C) + C_gH_g/C_o + C_fH_f/C_o = 0 \qquad . (19)$$

The nominal value of e_g is given by

$$e_g = V_F \qquad . (20)$$

Taking these auxiliary conditions into account, we now take the logarithmic

derivative of Eq. (4) and after some algebraic manipulation, obtain

$$\frac{\delta e_g}{e_g} = \frac{\delta V_F}{V_F} + \left[\frac{K(H_F + V_C)/V_F - 1)}{K - 1}\right]\frac{\delta C_o}{C_o}$$

$$+ \frac{K}{K - 1}\left[\frac{H_F + V_C}{V_F}\right]\frac{\delta K}{K} + \frac{C'_o}{(K - 1)C_o}\left[\frac{H_F + V_C}{V_F} - 1\right]\frac{\delta C'_o}{C'_o}$$

$$+ \frac{C_g}{(K - 1)C_o}\left[\frac{H_f}{F} - 1\right]\frac{\delta C_g}{C_g}\left[\frac{C_o + C'_o + C_f}{(K - 1)C_o}\right]\frac{\delta C_f}{C_f}$$

$$+ \frac{1}{K - 1}\left[1 + \frac{C'_o + C_g + C_f}{C_o}\right]\frac{\delta G}{G}$$

$$+ \frac{1}{(K - 1)C_o}\left[(KC_o + C'_o)\left(\frac{H_F}{V_F}\frac{\delta H_F}{H_F} + \frac{V_C}{V_F}\frac{\delta V_C}{V_C}\right) + \frac{C_f H_f}{V_F}\frac{\delta H_f}{H_f} + \frac{C_g H_g}{V_F}\frac{\delta H_g}{H_g}\right] \quad . \quad (21)$$

In interpreting Eq. (21) we must note that H_F and H_g are "transformer effect" hum voltages, and are therefore in time quadrature with the flow voltage V_F. Hence also, according to Eq. (19), V_C is in time quadrature with V_F. Therefore in Eq. (21) all terms with factors H_F/V_F, V_C/V_F, and H_g/V_F indicate that variations are caused in the time quadrature component of the signal, but do not cause any variation in the in-phase or signal phase of the measured voltage.

Let us examine the in-phase and quadrature phase terms of Eq. (21) separately. The in-phase or signal phase contributions to the error may be written, taking into account also the error derivatives of Eqs. (1) and (2).

Signal Phase Error for Volumetric Measurement

$$\frac{\delta e_g}{e_g} = -\left[\frac{K}{K-1}\frac{\delta E(\beta,1)}{E(\beta,1)} + \cot\beta\delta\beta\right]$$

$$-\left[\frac{1}{K-1}\frac{\delta L}{L} - \frac{\delta a}{a}\right] - \frac{C_o'}{(K-1)C_o}\frac{\delta C_o'}{C_o'}$$

$$+\left[\frac{C_o + C_o' + C_g + C_f}{(K-1)C_o}\right]\frac{\delta G}{G} - \frac{C_g}{(K-1)C_o}\frac{\delta C_g}{C_g}$$

$$+\frac{\delta B}{B} + \left[\frac{C_o + C_o' + C_f}{(K-1)C_o}\right]\frac{\delta C_f}{C_f} \qquad . \quad (22)$$

In Eq. (22) the terms in the first bracket on the right hand side of the equation depend only on errors in the angle β, which is the semi-angle subtended by the curvilinear detection electrode. It is not expected that this angle will change significantly with internal pressurization of the transducer tube or because of shrinkage due to cool-down from the thermal shock of LH_2.

The terms in the second bracket on the right hand side of Eq. (22) involve dimensional tolerances or variations in the transducer tube. The interior radius of the tube a may be expected to increase in direct proportion to fluid pressurization (the fiberglas wall is designed to strain a maximum of 0.1 percent under an anticipated internal pressurization of 1,000 psi). During cool-down to LH_2 temperatures both the length L of the detection electrode and the interior radius a of the transducer tube may be expected to decrease; and for fiberglas the shrinkage to LH_2 temperatures is in the neighborhood of 0.2 percent. Because of the coefficient $1/(K-1)$, the term $\delta L/L$ is the most significant term. It indicates that there may be a calibration error of somewhat less than one percent during the ex-

tremely brief period of time it takes for the detection electrode to shrink to its equilibrium value.

The term $\delta C_o'/C_o'$ indicates an error due to variation in the fringe capacitance C_o'.

The terms in the third bracket on the right in Eq. (22) correspond to errors caused by gain variations in the transducer amplifier. In the flowmeter transducer amplifier there is more than 55 db of feedback, and it is therefore expected that $\delta G/G$ can be kept to less than something like 1/5000. Under these conditions the terms in the third bracket can be kept to less than the order of one percent in the volumetric mode of operation.

Hum or Quadrature Phase Error for Volumetric Measurement

$$\frac{\delta e_g}{e_g} = \frac{K}{K-1}\frac{(H_F + V_C)}{V_F}\left[\frac{\delta K}{K} + \frac{\delta C_o}{C_o}\right] + \frac{H_g}{V_F}\frac{C_g}{(K-1)C_o}\frac{\delta C_g}{C_g}$$

$$+ \frac{C_o'}{(K-1)C_o}\left[\frac{H_F + V_C}{V_F}\right]\frac{\delta C_o'}{C_o'}$$

$$+ \frac{1}{(K-1)C_o}\left[(KC_o + C_o')\left(\frac{H_F}{V_F}\frac{\delta H_F}{H_F} + \frac{V_C}{V_F}\frac{\delta V_C}{V_C}\right) + \frac{C_f H_f}{V_F}\frac{\delta H_f}{H_f} + \frac{C_g H_g}{V_F}\frac{\delta H_g}{H_g}\right]. \quad (23)$$

All of the terms in Eq. (23) essentially indicate that the quadrature voltage or hum can be expected to vary when any one of the parameters in the electromagnetic flowmeter varies. This equation points up the great advantage in mechanically shimming the pertinent electrical circuitry so as to make the inherent hum voltages H_F, H_g, and H_f as small as possible, and so that by Eq. (19) V_C is also small. In other words, it is advantageous to have the necessary mechanical vernier adjustments on the electrode circuitry so that, in each and every transducer tube, the hum voltages H_F, H_g, and H_f are maintained at an adequately small value.

Eqs. (22) and (23) also indicate that large vapor bubbles (which cause the bulk dielectric constant to approach unity) cause considerable upset to the flowmeter.

B. Massmetric Mode

For the electromagnetic induction flowmeter operating in the massmetric mode, the in-phase and hum phase error relationships are as follows.

Signal Phase Error for Massflow Measurement

$$\frac{\delta e_g}{e_g} = \left[\frac{2}{K+2}\frac{\delta L}{L} - \frac{\delta a}{a}\right] + \left[\cot\beta\delta\beta - \frac{K+4}{K+2}\frac{\delta E(\beta,1)}{E(\beta,1)}\right] - \left[\frac{C_o'\delta C_o'/C_o' - C_g\delta C_g/C_g + (2C_o - C_o' - C_g)\delta C_f/C_f + (2C_o - C_o' - C_g - C_f)\delta G/G}{(K+2)C_o}\right] + \frac{\delta B}{B} \quad ; \quad (24)$$

Hum or Quadrature Phase Error for Massflow Measurement

$$\frac{\delta e_g}{e_g} = \frac{K}{K+2}\left[\frac{H_F + V_C}{DF_m}\right]\left[\frac{\delta K}{K} + \frac{\delta C_o}{C_o} + \frac{C_o'}{KC_o}\frac{\delta C_o'}{C_o'}\right] + \frac{H_g}{DF_m}\frac{C_g}{(K+2)C_o}\frac{\delta C_g}{C_g} + \left[\frac{KC_o + C_o'}{(K+2)C_o}\right]\left[\frac{H_F}{DF_m}\frac{\delta H_F}{H_F} + \frac{V_C}{DF_m}\frac{\delta V_C}{V_C}\right] + \frac{C_g}{(K+2)C_o}\frac{H_g}{DF_m}\frac{\delta H_g}{H_g} + \frac{C_f}{(K+2)C_o}\frac{H_g}{DF_m}\frac{\delta H_f}{H_f} \quad . \quad (25)$$

The discussion bearing on Eqs. (24) and (25) is similar to that for volumetric flowmeter analysis. We note, however, that there is a very considerable difference in performance in that for the volumetric flowmeter most of the error terms contain

(K - 1) in the denominator; whereas in the massflow error analysis these terms are generally replaced by (K + 2). When a fluid such as LH_2, with a low dielectric constant, K, is employed, this makes a very noticeable difference. It is to be noted, therefore, that the electromagnetic flowmeter operating in the massmetric mode has considerably less error involved and there is no great upset attendant to the passage of large vapor bubbles. Indeed, if the vapor bubbles are macroscopically uniform in their distribution (e.g., like a foam), the EM massflowmeter responds properly to their massflowrate. Other notable features are also evident from Eq. (24): we no longer have the same transient error while the length of the detection electrode L shrinks to its equilibrium value; also we see that errors due to gain stability in the transducer amplifier are very considerably less--and indeed, now are quite negligible--in the massflow mode of operation.

C. Phase-Sensitive Detector Error

The foregoing analysis has indicated that the various elements and components in the electromagnetic flowmeter contribute to the overall error or variation in the flowmeter signal e_g. This flowmeter voltage e_g consists of a flowrate signal component e_{gf} and a quadrature or hum voltage e_{gh},

$$e_g = e_{gf} + ie_{gh} \quad , \quad (26)$$

where we use complex notation, with $i = \sqrt{-1}$.

Now, the phase-sensitive detector is nominally established to detect the flow signal component voltage and reject the quadrature or hum component or voltage. Thus the output of e_o of the phase-sensitive detector can be expressed by

$$e_o = e_{gf} \cos \theta + e_{gh} \sin \theta \quad , \quad (27)$$

where the nominal or ideal value of θ is

$$\theta = 0 \quad . \quad (28)$$

Taking the logarithmic error differential of Eq. (27), and using the auxiliary Eq. (28), we find

$$\frac{\delta e_o}{e_o} = \frac{\delta e_{gf}}{e_{gf}} + \frac{e_{gh}}{e_{gf}} \delta\theta \qquad . (29)$$

The first term on the right of Eq. (29) is essentially the error in flow voltage as already discussed above.

The second term on the right side of Eq. (29) indicates that a flow signal error will exist if the phase-sensitive detector is not perfectly aligned so as to accept the flow signal and reject the hum voltage. We see that the coefficient of this phase angle detection error $\delta\theta$ is e_{gh}/e_{gf} where the denominator is the magnitude of the flow signal and the numerator is the nulled (by means of the compensation voltage V_C) value of the hum voltage. Thus if the nulled value of the hum voltage e_{gh} is maintained at a small value relative to the flow signal, we see that slight errors in the phase setting of the phase-sensitive detector are not serious. But if the nulled value of e_{gh} is equal to the difference of a large inherent hum voltage and an equally large compensation voltage V_C, then we may expect--and indeed we have observed--that the "nulled" value of e_{gh} drifts away (because of thermally induced changes in certain critical electrical capacities within the transducer tube), and quite soon becomes large relative to e_{gf}; and a slight error in setting of the phase-sensitive detector then allows an appreciable component of this hum to be sensed as a flow signal. It is thus important to see that the inherent hum in the transducer tube is mechanically adjusted to a small value so that variations (due to temperature change in certain transducer interelectrode capacitances) in the nulled value of e_{gh} can be maintained small. Alternatively, an automatic means for continuously nulling e_{gh} may be employed.

V. TEST PROCEDURES AND TECHNIQUES

The operation of the electromagnetic flowmeter will be described in this Section. In particular we will discuss the various controls available to the operator and summarize the experimental results obtained from flow test runs in liquid hydrogen.

A. Operation

The control available on the present model flowmeter is far more versatile than need be for the usual flow measurement requirements. However, such versatility in control was extremely useful during the developmental stages of the instrument.

To prepare the electromagnetic flowmeter for a flow test run, set the driven-shield electrode voltage for operation in either the mass-metric mode or volumetric mode, and introduce a voltage at the compensation electrode to null the "transformer effect" voltage. After this two-step process the flowmeter is ready for operation.

These two steps are accomplished as follows (Refer to Fig. 3 on Page 23):

(a) Mount the flowmeter in the line.

(b) Connect cables between control cabinet and flowmeter. The cable connections are shown in Fig. 4.

(c) Turn on power switch and allow 30 sec for warm-up; then turn on B+ supply voltage.

(d) Turn the Run-Off-Cal switch to the Cal position.

(e) Turn the Norm-Comp switch to the Comp position.

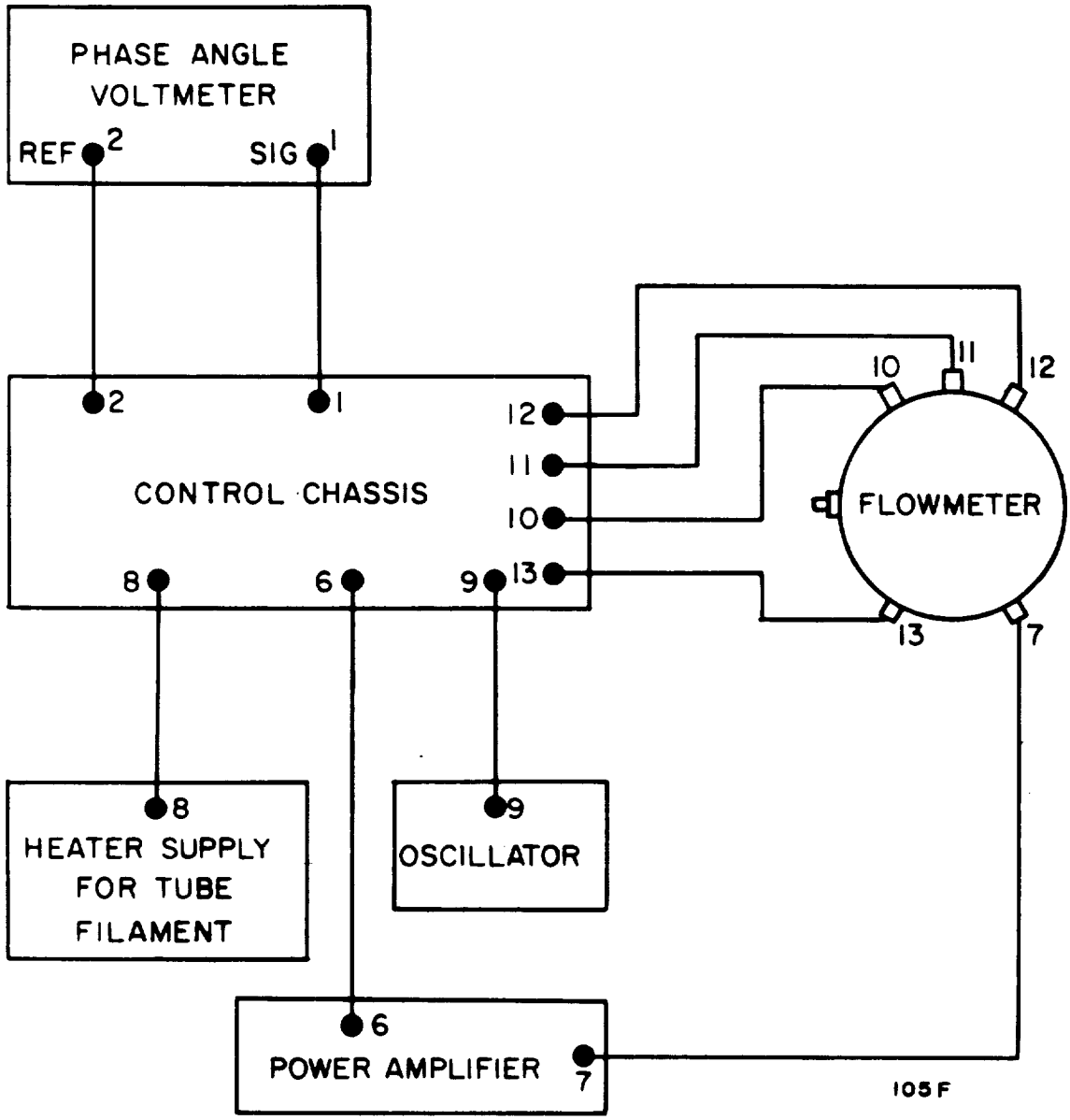

Fig. 4 Cable connections between flowmeter and control cabinet. All cables are marked at both ends with the numbers shown. Interconnecting 60 cycle power cables are also labeled but are not shown in this diagram. Cables transmit voltages and power as follows:

1. Processed signal
2. Processed reference
6. 10 kc input to power amplifier
7. Magnet power
8. Filament power
9. 10 kc input to control chassis
10. Compensation
11. Filament and B+ supply
12. Signal output from preamplifier
13. Reference

(f) Measure the amplitude and the phase of the voltage at the output of the compensation amplifier with the phase-angle voltmeter.

(g) Turn the Norm-Comp switch to the Norm position.

(h) Adjust the driven-shield phase control until the phase of the signal, e_g, is in the exact same phase as V_C, the voltage which was sensed when the Comp-Norm switch was set in the Comp position.

(i) The amplitude control is then adjusted so that e_g/V is as required either for volumetric or massflow operation as described in subsections D, E, and F of Section II. [In particular see Eqs. (9) and (17) for the respective volumetric and massmetric gain settings.*]

(j) Turn the Run-Off-Cal switch to the Run position.

(k) Set the phase-angle voltmeter to detect signals in phase with the hum voltage (i.e., in phase with the voltage output of the reference loop).

(l) Adjust the amplitude control and phase shift control until a null is obtained. The compensation of the hum voltage is now complete.

(m) Set the phase-angle voltmeter so as to sense signals in quadrature with the reference voltage.

---

*The controls on the present flowmeter allow one to set the degree of positive feedback to drive the driven shield at the gain desired. This variable gain feature is not an essential one since at present it appears that only two specific feedback settings (for the massmetric or volumetric mode of operation) are of interest. Therefore, while the manipulations described are now required the controls could be reduced to a two-position switch, one position for massmetric operation, the other for volumetric operation.

B. Experimental Results

The main objectives of the experimental effort to date have been to determine:

1. That the mechanical design is compatible with the environment attendant to a liquid hydrogen flow system [and specifically, the flow system of the Lewis Research Center (LeRC) LH_2 flow test facility];
2. That a flow signal (which has already been obtained with oil, which has a dielectric constant of 2.2; and with LN_2 which has a dielectric constant of approximately 1.5) can be obtained under the electrically more difficult conditions of LH_2 with its low dielectric constant of approximately 1.25;
3. That the flow signal is linear with the flow rate.

From the data we present in this subsection we shall see that the electromagnetic flowmeter has successfully met all of these test objectives.

From the discussion in Section II above we know that the present design electromagnetic flowmeter must be expected to have a zero point drift because of dielectric constant changes in the transducer tube which are associated with temperature drift toward thermal equilibrium; and we realize that with the rigid geometry of electronic circuitry in the present type of transducer tube we may occasionally find an undesirably high magnitude of hum. The hum can be bucked out with a compensation voltage, but if the hum voltage happens to be high, so that the compensation voltage must be correspondingly opposite in phase and equally high, we must depend upon

the phase and amplitude stability of these two large voltages to maintain the null. In the present LH_2 electromagnetic induction flowmeter the observed zero point drift is qualitatively in agreement with the theory described in Section IV above in its dependence on thermal changes and its dependence on compensated null stability.

Some difficulty was encountered in connecting the ring demodulator of the North Atlantic phase angle voltmeter to the input of the Speedomax recorder at the LeRC liquid hydrogen test facility. As a result the circuits for the Speedomax recorder input and the phase-angle voltmeter output were carefully studied, and it was determined that the two input terminals to the recorder, although both off ground, were not equally balanced and that the resulting unbalance caused improper operation of the ring demodulator in the phase-angle voltmeter. It was decided that a more balanced condition could be obtained by the use of a fairly simple passive circuit, shown in Fig. 5, along with the ring demodulator output circuit of the phase-angle voltmeter and the input circuit of the recorder. All subsequent flowmeter runs were made using this passive circuit with the phase-angle voltmeter set in the 0.001 position and the recorder set in the 5 millivolt position. Since the recorder had two recording pens, the output of the electromagnetic flowmeter was used to drive one pen and the output of a turbine Pottermeter was used to drive the other pen.

The EM flowmeter was connected into the LH_2 line at the LeRC test facility as shown in Fig. 6.

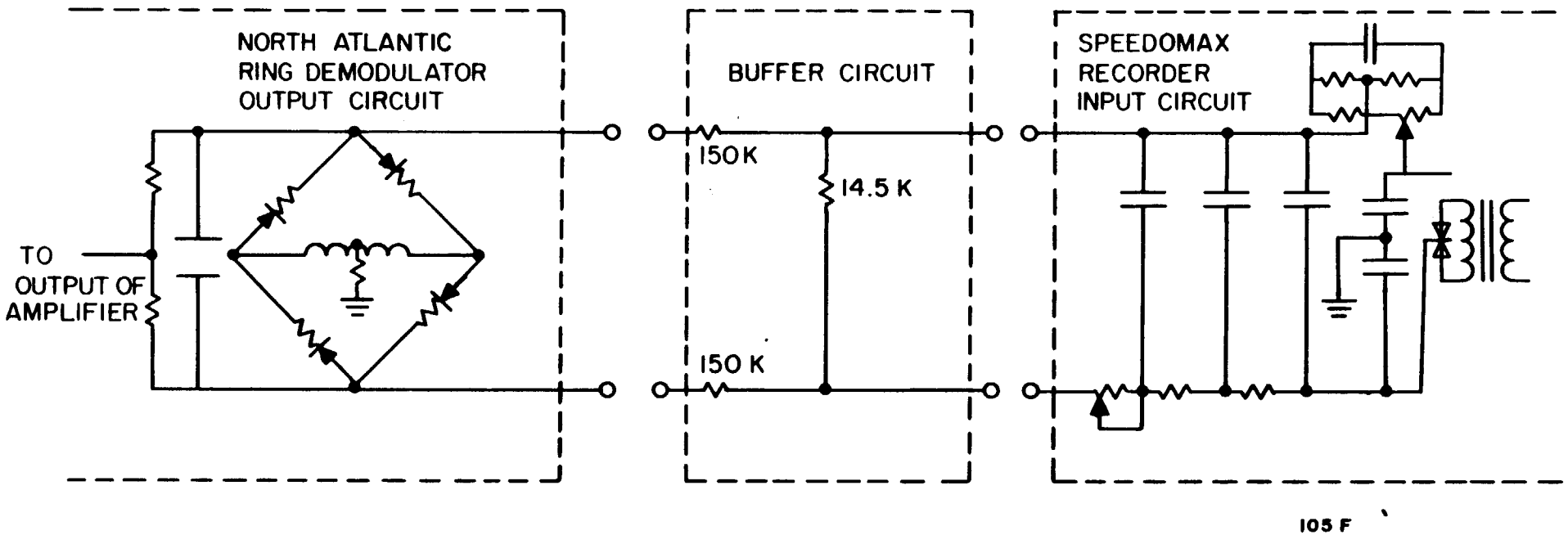

Fig. 5 Output circuit of the North Atlantic phase-angle voltmeter and input circuit of the Speedomax recorder. Also shown is buffer circuit used to obtain isolation between the two circuits. This buffer circuit was necessary to prevent adverse effects on the ring demodulator. All Speedomax records were obtained using this circuit.

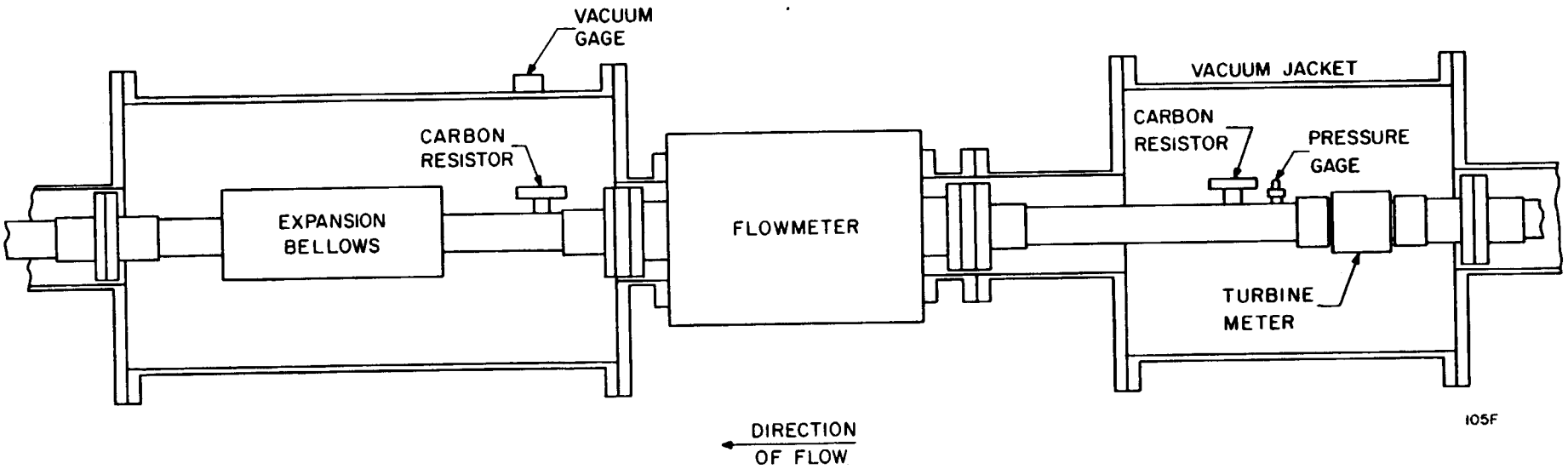

Fig. 6 Connection of the EM flowmeter into the LH_2 line of the LeRC test facility.

Figures 7 and 8 present data showing the linearity of the volumetric signal output of the electromagnetic flowmeter for LH_2 flowrates from 20 gpm to 100 gpm*. Figure 7 is a Speedomax strip chart reproduction showing the comparative signal outputs of the electromagnetic flowmeter and a standard Pottermeter Model 1-1/2-5440B turbine meter. Figure 8 is a linearity plot of the electromagnetic flowmeter signal outputs versus the Pottermeter signal outputs shown in Fig. 7.

Figures 9 and 10 present data showing the linearity of the massmetric signal output of the electromagnetic flowmeter for LH_2 flowrates from 20 gpm to 80 gpm. Figure 9 is a strip chart reproduction showing the comparative massmetric signal outputs of the electromagnetic flowmeter and the volumetric signal outputs of a standard Pottermeter Model 1-1/2-5440B turbine meter. Figure 10 is a linearity plot of the electromagnetic flowmeter signal outputs versus the Pottermeter signal outputs shown in Fig. 9.

From the records shown in Figs. 7 through 10, we see that the evidence of linearity in the EM flowmeter is excellent; since the Pottermeter has a dynamic range of only about 2:1, we cannot expect to see better performance. In fact, runs below 20 percent of full flowrate are not usually made because the Pottermeter tends to stick in the lower range. In the experimental set-up leading to the records shown in Figs. 7a and 8a, no effort had been made to adjust the scale of the EM flowmeter output to that of the Pottermeter, and the difference in scales is obvious; however, the evidence bearing on linearity was obtained.

---

*More precisely, from 20 percent to 100 percent of full flow; full flow is approximately one pound per second of LH_2 or approximately 103 gpm.

In respect to the drift in the present LH_2 electromagnetic flowmeter we refer to Eq. (8) above, which shows how the ratio e_g/V_C depends on the various capacities, and most importantly, depends on the capacity C_f between the driven-shield electrode and the detection electrode. We know from independent measurements that C_f decreases as the temperature of the fiberglas decreases, and from room temperature down to liquid hydrogen temperature the variation can be in the order of 10 percent. Since the fiberglas, which serves as the dielectric material between the driven-shield electrode and the detection electrode, is dimensionally fairly stable (from independent tests it is known to shrink during cool-down to LH_2 temperatures by 0.2 to 0.3 percent) we know that the observed decrease in capacity must correspond not to a decrease in dimension, but rather to the decrease in dielectric constant as the fiberglas cools down to LH_2 temperatures. Since the quantity (1 - G) in Eq. (8) is a negative number, we must expect the denominator in Eq. (8) to become larger and larger as C_f falls during the process of cool-down; and hence we must expect the ratio e_g/V_C to fall during the process of cool-down. The ratio e_g/V_C is obtained--as described in Section II B--by shutting off the magnet so that the flow voltage and all hum voltages go to zero, and then injecting a known constant voltage V_C into the compensation electrode.

Measurements of the variation of e_g/V_C between room temperature and liquid hydrogen temperature were made on the LeRC flow test facility. This was done by cooling the meter to LH_2 temperature until thermal equilibrium was attained within the flowmeter. The flowmeter was emptied of liquid and the value of e_g/V_C was recorded as 6.05. After the flowmeter had reached room

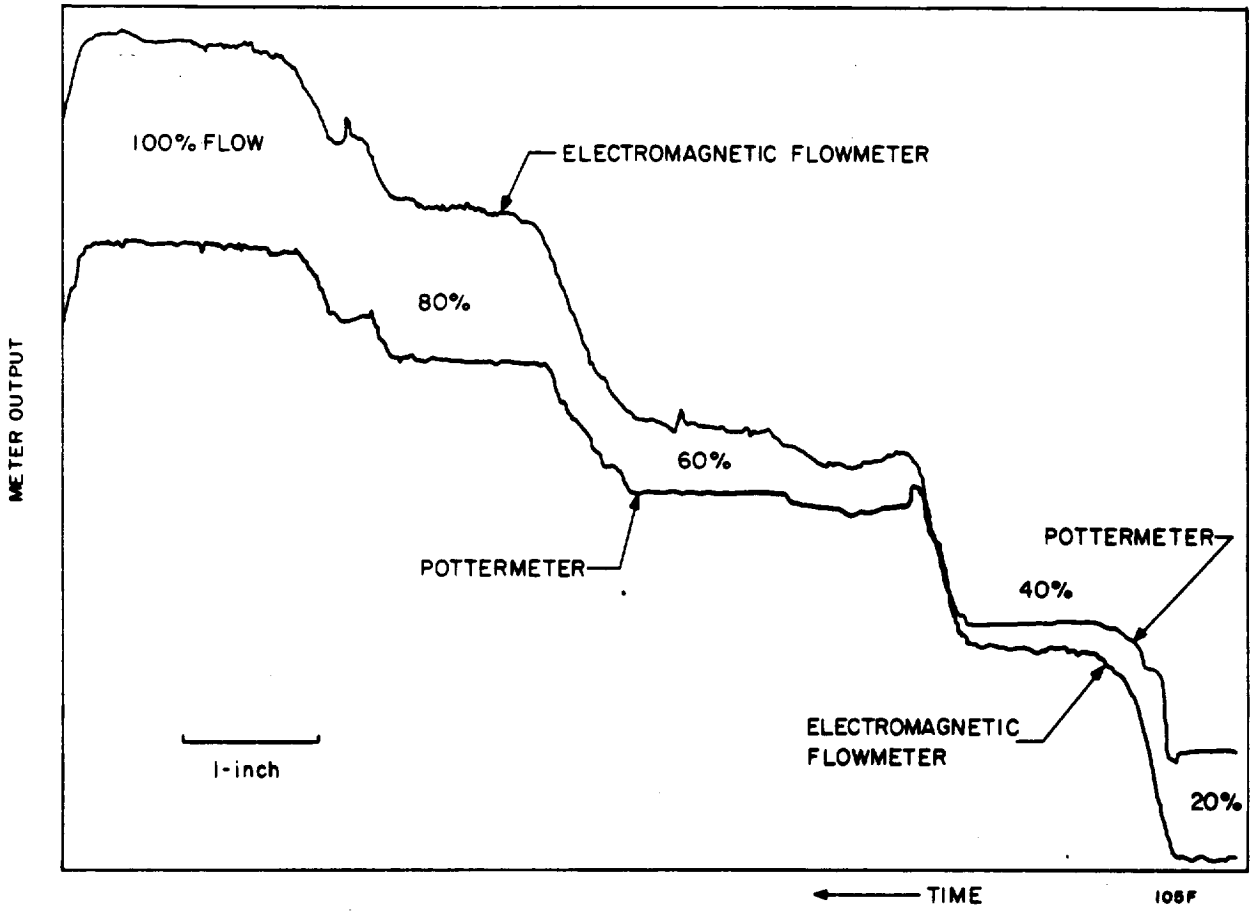

Fig. 7 Strip chart recording comparing the volumetric flow signal outputs of the LH_2 electromagnetic induction flowmeter and a standard Pottermeter Model 1-1/2-540B turbine meter. Comparative signal outputs are shown for different flowrates given as percents of full flow. Full flow is 1 pps of LH_2. No attempt was made to make the output signals of the two meters equal.

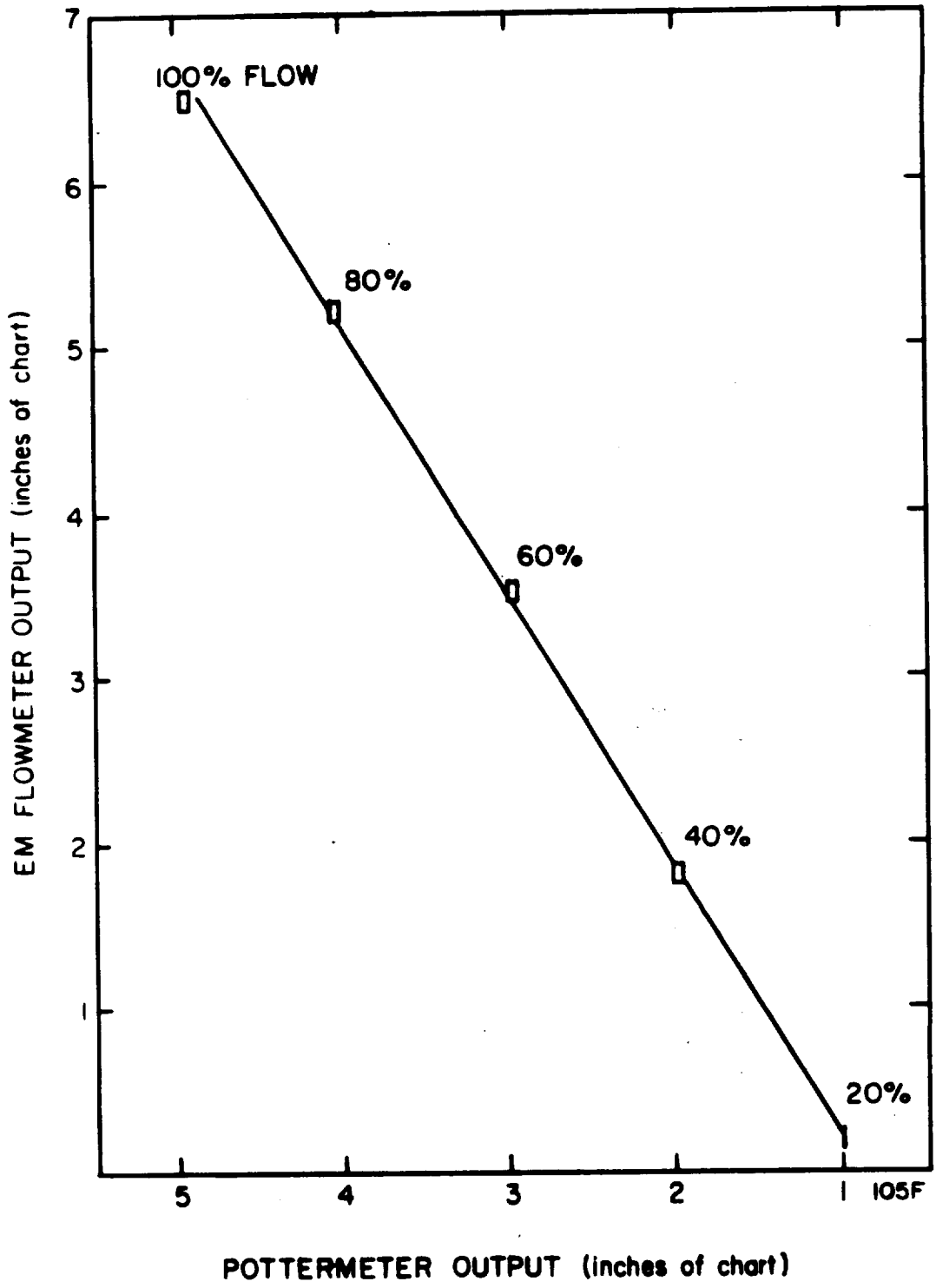

Fig. 8 Linearity plot of strip chart recording shown in Fig. 7. The range of values for smoothed data taken over relatively constant flow rates (given as percents of full flow) is indicated by the rectangles. A visually determined best straight line is drawn through the experimental data.

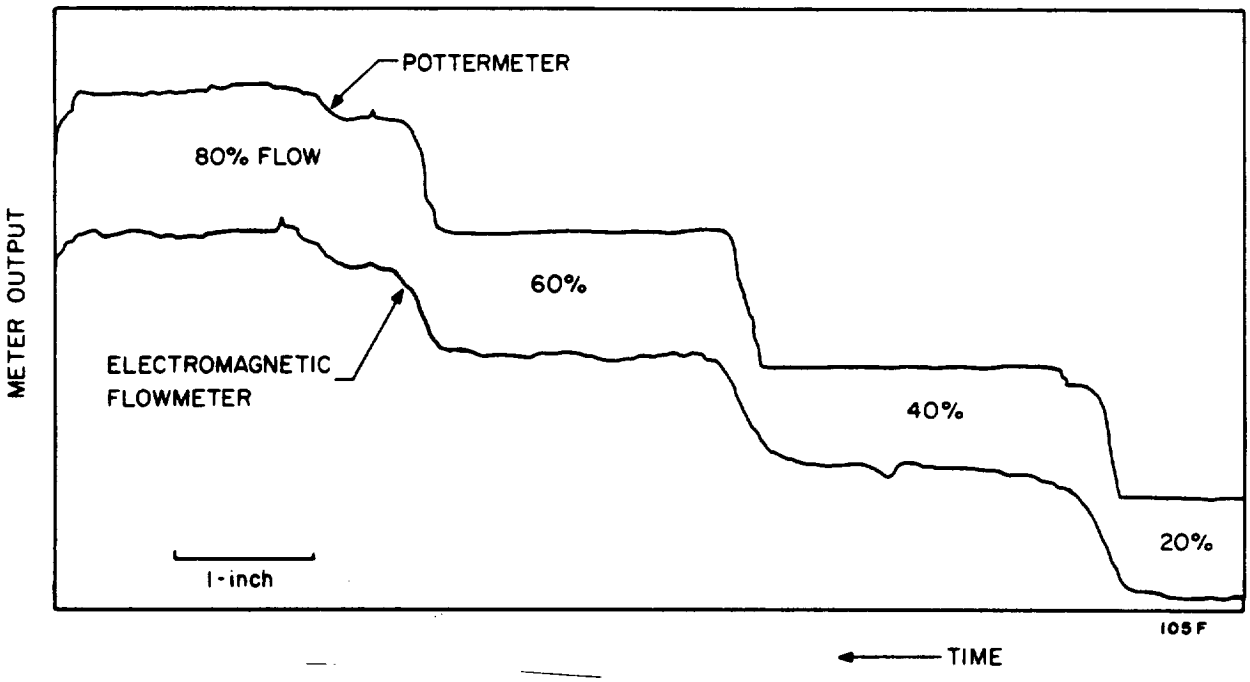

Fig. 9 Strip chart recording comparing the mass flow signal output of the LH_2 electromagnetic induction flowmeter and the volumetric flow signal output of a standard Pottermeter Model 1-1/2-5440B turbine meter. Comparative signal outputs are shown for different flowrates given as percents of full flow. Full flow is 1 pps of LH_2. No attempt was made to make the output signals of the two meters equal.

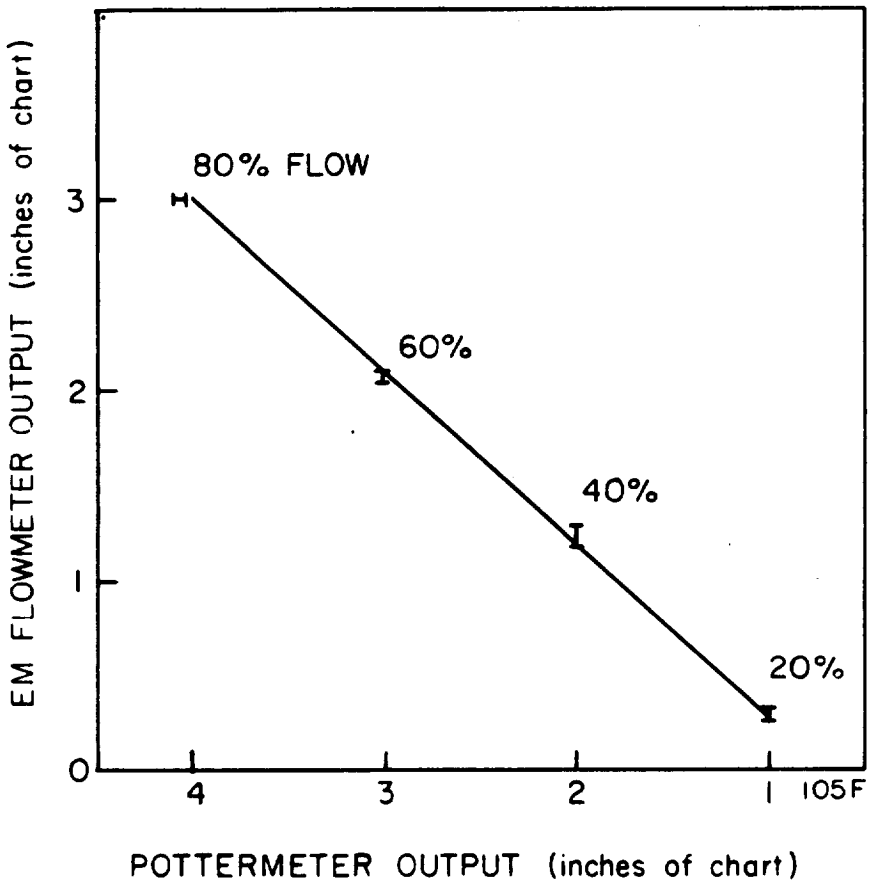

Fig. 10 Linearity plot of strip chart recording shown in Fig. 9. The I symbols denote the range of the smoothed experimental data taken over relatively constant flow rates (given as percents of full flow). A visually determined best straight line is drawn through this data.

temperature the value of e_g/V_C was 7.25. The direction of change of these values with temperature is as indicated by Eq. (8).

Consideration of Eq. (4) above shows that not only the calibration constant of the flowmeter must be expected to change during cool-down, but also that the effect of the several hum generators--H_F, H_g, H_f--must be expected to vary, ultimately reaching a magnitude (unless the compensation voltage V_C is continuously adjusted) where the linearity of the phase-sensitive detector is compromised. When this happens a drift in the zero point of the flow signal becomes apparent.

Rather early in the test runs it was noted that approximately one-half hour was needed before the flowmeter reached a temperature equilibrium such that flowrate measurements could be made without complications of drift. To establish qualitative information on zero point drift a record was made on a Speedomax recorder from the time cold gas entered the flow test section until the resistive temperature gages in the flow test section indicated liquid hydrogen temperatures. Both the hum phase and the signal phase were recorded.*

The hum phase is particularly sensitive to this cool-down process, and the signal phase is relatively insensitive to the cool-down.

The sensitivity of the hum voltage with cool-down suggests that changes in the dimensions of the transducer tube bring about changes in the effective

---

*One should realize when reviewing this data that the cool-down process was not a continuous one. The liquid hydrogen flow through the transducer tube could be maintained for two minute periods only; then the flow had to be stopped, reversed, stopped again, then restarted. Under these conditions it was difficult to obtain quantitative data during the cool-down period.

area of the loop responsible for the transformer effect on hum voltage. Fig. 11 shows a plot of both the signal phase and the hum phase of the electromagnetic flowmeter output as a function of time in inches of chart.

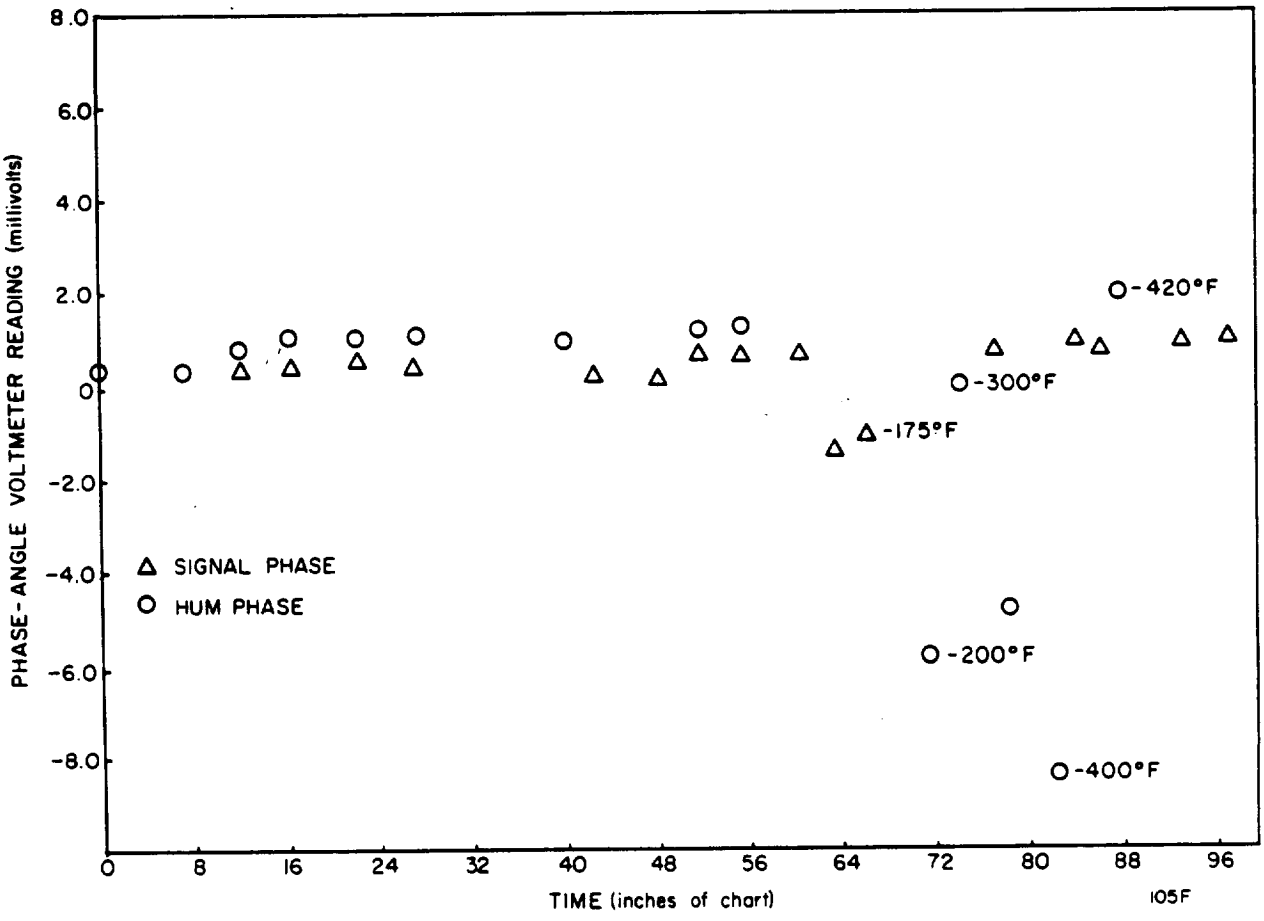

Fig. 11 Phase angle voltmeter readings vs. time. This figure indicates the drift in the signal and hum phases from the time cold gas entered the flow test section until the resistive temperature gage in the flow test section indicated the presence of liquid hydrogen. The signal phase is relatively insensitive to cool-down compared to the hum phase. Several of the points are identified by the temperature of the test section. Chart speed was one inch every 7.14 seconds.

VI. CONCLUSIONS AND RECOMMENDATIONS

Under contracts NASr-13 and NASr-53, the Engineering-Physics Company carried out for the National Aeronautics and Space Administration an engineering analysis and experimental verification of an electromagnetic flowmeter which would be operable with dielectric fluds. Then, under contract NASw-381, the EPCO staff embellished this earlier effort, culminating in the fabrication and test of such an induction flowmeter for use with liquid hydrogen plumbing systems. The following notable virtues of the electromagnetic induction flowmeter have been practicably attained:

1. Obstructionless--no pressure drop;
2. No moving parts;
3. Linearity over a wide dynamic range--including flow in either direction;
4. Excellent sensitivity to flow variation or flow oscillation;
5. Volumetric flow measurement which is insensitive to the fluid's electrical properties or variations thereof; and in the same instrument, by an alternate adjustment of a preamplifier gain setting;
6. Massmetric flow measurement for non-polar fluids (regardless of phase) such as the cryogenic propellants;
7. Self-calibration capability in the field.

Sufficient conditions for the proper operation of the electromagnetic flowmeter are: (1) the flow velocity profile must be symmetric with respect

to the axis of the flowmeter; (2) the electrical properties of the metered fluid must be macroscopically uniform throughout the sensing section of the electromagnetic flowmeter. For a two-phase fluid in the massmetric mode, the latter condition implies that such a mixture must be something like a foam; however, the quality of the foam may vary between zero and one. Whether and to what degree of accuracy the electromagnetic flowmeter will operate with stratified two-phase mixtures is a subject which requires further research. Meantime, if highly stratified two-phase flow is a matter of serious importance, the user of the EM flowmeter should establish some kind of an homogenizer (e.g., a turbulence screen) upstream of the flow sensing section.

The experimental success reported herein with this flowmeter has at the same time indicated that the present electronic and mechanical configuration of the EM induction flowmeter gives rise to temperature sensitivity; consequently the present configuration is workable only after thermal equilibrium has been achieved. Once this temperature sensitivity has been eliminated or adequately minimized, the electromagnetic induction flowmeter will be useful even in the face of thermal shock associated with cool-down to cryogenic temperatures. It is therefore recommended that the present design of the electromagnetic induction flowmeter be modified both electronically as well as mechanically--including the use wherever possible of temperature insensitive constructional materials such as quartz--to render the electromagnetic flowmeter adequately insensitive to temperature variations associated with thermal shock.

Appendix A

MECHANICAL DESIGN

I. INTRODUCTION

The electromagnetic flowmeter developed by the Engineering-Physics Company for use with cryogenic fluids consists of several subassemblies. These subassemblies are discussed in detail in subsequent appendices.

II. GENERAL DESIGN

Figure A1 shows the final flowmeter configuration.

The heart of the flowmeter is the transducer tube which has several electrodes embedded in a fiberglas tube.* The transducer tube is the structural member which contains the fluid pressure and maintains the electrodes in a fixed relationship to one another.

Separating the transducer tube from the cryogenic fluid is an impermeable plastic liner (Kel-F). This liner is flared at each end to form a gasket-type seal which is captured between metal flanges. These metal flanges form the exposed ends of the flowmeter and are suitable for use with a soft metal gasket.

Surrounding the transducer tube is an area of high vacuum which provides for thermal insulation of the transducer tube. The flowmeter is arranged so that when connected to a vacuum-jacketed fluid line, the vacuum is maintained within the flowmeter, in the space between the transducer tube and the flowmeter vacuum jacket. This vacuum jacket is fabricated of Delrin (an Acetal resin supplied by E. I. du Pont de Nemours and Co.)

---

*Gilbert Plastics and Supply Co., Panelyte Grade 160, NEMA Grade G10, MIL-P-18177 GEE. This is a glass cloth based laminate with epoxy resin; it has high mechanical strength.

Wrapped around the vacuum jacket is the cosine wound magnet coil used to establish a uniform magnetic field in the transducer tube. A magnetic core is positioned around the coil to minimize the reluctance of the overall magnetic circuit.

The assembly thus far described is contained in an aluminum housing which is the main structural member of the flowmeter. Separable end plates bolt to the aluminum housing and provide the means to affix and position the magnet coil, the Delrin vacuum jacket, the transducer tube, and the end flanges. These separable end plates also provide surfaces for connecting the line vacuum jackets, and they seal the magnet coil chamber from the vacuum and also allow it to be pressurized with helium if desired for safety reasons. The aluminum housing is shaped like a spool around which the flowmeter electronics are placed. The electronics are protected by a thin, removable aluminum cover. This cover mates with a stationary sleeve containing hermetically sealed electrical bulk-head connectors. There are five connectors arranged around the periphery of the flowmeter.

The chambers containing the electronics and the magnet coil are sealed, and means are provided for pressurizing these chambers to two atmospheres pressure of an inert gas such as helium. This is a safety feature to insure that an explosive mixture of hydrogen cannot accumulate in this experimental model.

Figures A2a and A2b show the flowmeter in the Engineering-Physics Company liquid nitrogen test circuit. (The cylinders with bellows at either end of the flowmeter are part of the line vacuum system and not part of the

flowmeter.) Figure A2a shows the flowmeter with the cover removed so that the electronics is exposed. In Fig. A2b the cover is in place and ready to be pressurized with helium.

III. SPECIFIC DESIGN DETAILS

The vacuum jacket is made of plastic since metal would be impermeable to the high frequency magnetic field. This jacket has a sleeve-type seal at either end where it mates with and is held by the separable end plates. Sealing is accomplished by the use of O-rings in conjunction with room temperature vulcanizing silicone rubber (RTV-102). The RTV-102 is used to bond together and to seal the jacket and the end plates. RTV-102 is an adhesive/sealent with a remarkable ability to adhere to most metals and plastics. It is supplied by General Electric Co., and a similar product is supplied by Dow Corning under the designation RTV-732. The silicone rubber sealent is used to compensate for any loosening of the O-ring seal which may be caused by differential expansion at low temperatures. The tenacious adherence of the rubber helps it to maintain intimate contact with both the vacuum jacket and the end plates at low temperatures. Since there is only a very slight radial clearance between the jacket and the end plates, permeability of helium through the rubber sealent and into the vacuum chamber is not a problem. However, permeability of the helium through the Delrin jacket wall appeared likely to be a problem. To eliminate this possibility the OD of the cylinder is wrapped with several layers of Mylar film which are epoxied in place.

To reduce the heat leak from the liquid hydrogen line to the flowmeter housing, bolts machined from Delrin were used to hold the outer conical end

flange firmly against the strain reliever at the end of the transducer tube. The Delrin bolts were used in place of steel, since a heat transfer calculation indicated a maximum heat loss of approximately 77 Btu/hr using six stainless steel bolts at each end of the flowmeter versus 3 Btu/hr using Delrin bolts.

The triax connectors pass through the Delrin vacuum jacket. To facilitate sealing the connectors, two 3/4-inch diameter Delrin sleeves (see Fig. C-1 in Appendix C) are screwed into the vacuum jacket wall. The triax connectors seal on the inside diameter of the sleeves with neoprene O-rings. The sleeves are sealed to the jacket by applying an epoxy (Hysol 4183 resin with hardener 3485) to the screw threads and curing it in place. The vacuum jacket and the 3/4-inch diameter sleeves are wrapped with a ground shield, designed to be permeable to the 10 kc alternating magnetic induction while electrostatically shielding the flow sensing circuitry from the electric voltages applied to the magnet coil. The shield is formed by wrapping 0.005 inch diameter insulated magnet wire around the jacket and sleeves. Each loop of wire touches but does not overlap the adjoining loop. An epoxy adhesive is applied to the Delrin jacket and sleeves prior to the wire wrapping. After the jacket and sleeves are completely covered, the epoxy is cured, thus holding the wire in place. A bus bar is soldered to each wire loop along the jacket and sleeve lengths. This is accomplished by machining a slot, 0.002 inches deep, in each loop. This removes the insulation and permits the bus bar to be soldered in place. Diametrically opposite from the bus bar, a 1/32-inch wide slot is cut through each loop. This insures that no

conducting loops are present to set up eddy currents. The bus bar is then connected to the flowmeter housing.

The electronic components are mounted on terminal boards fastened to a 0.020 inch thick aluminum chassis contoured to fit over the curvature of the flowmeter housing. The chassis is insulated by Teflon covered with Mylar. The chassis is fastened to circular rings (not shown in Fig. A1) which clamp around the housing and thus eliminate the need for tapping into the housing wall which also serves as an electromagnetic shield to contain the magnetic lines of flux. The chassis was originally shock mounted, but it was found that this is unnecessary.

All O-rings are neoprene compound C-147-7. The widths of all grooves are reduced from the standard dimensions suggested by the Parker Seal Company. The narrower grooves minimize the pumping action of the O-ring and insure more positive sealing.

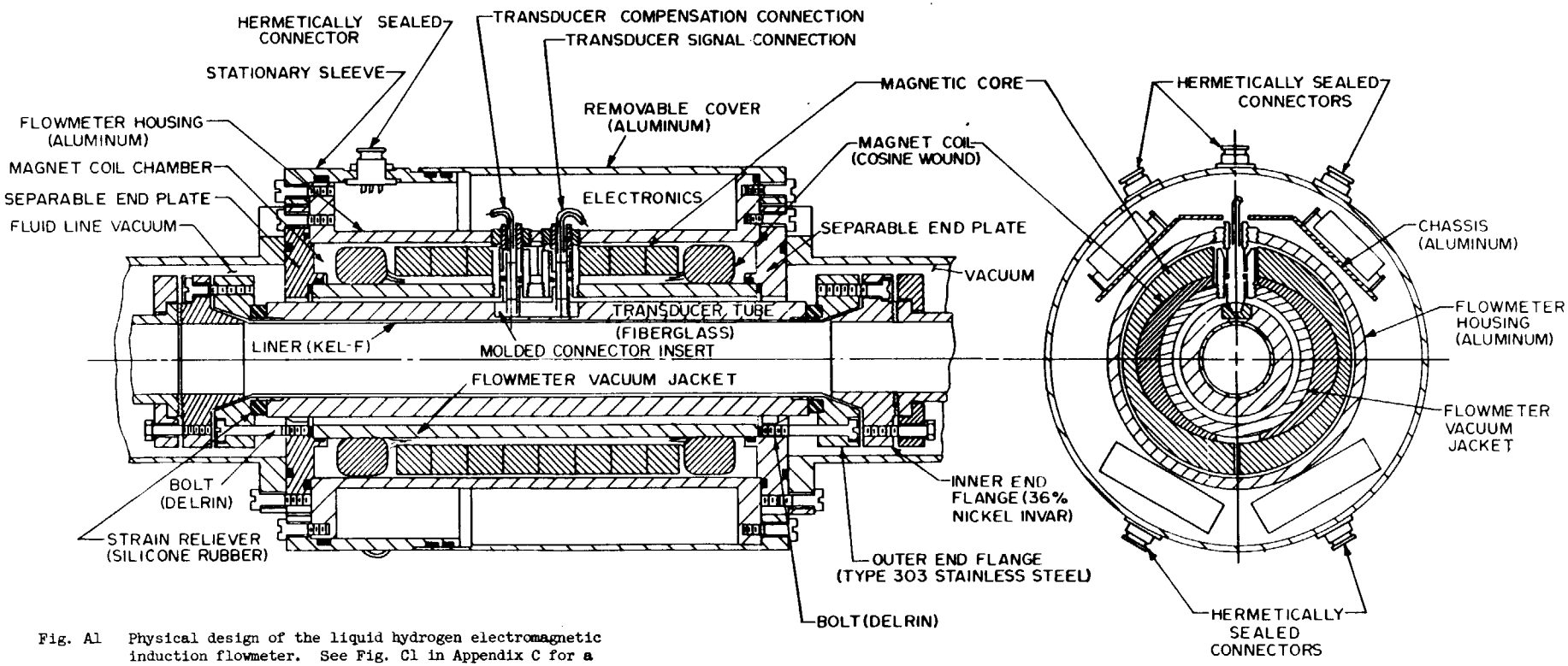

Fig. A1 Physical design of the liquid hydrogen electromagnetic induction flowmeter. See Fig. C1 in Appendix C for a detailed drawing of the triax connector.

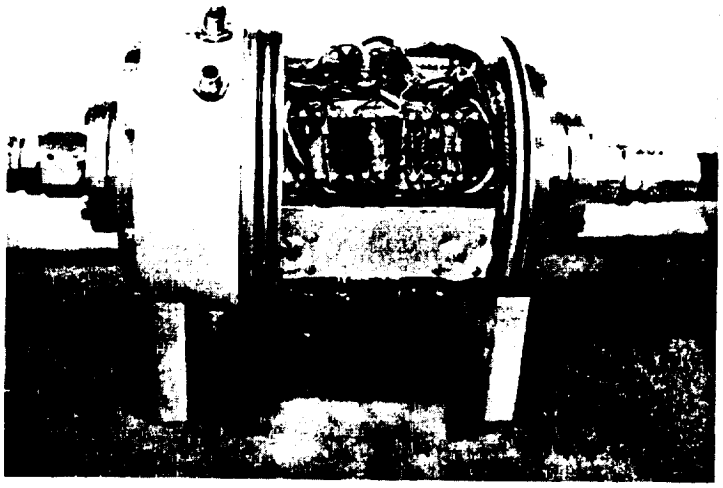

(A2a) Flowmeter with cover removed.

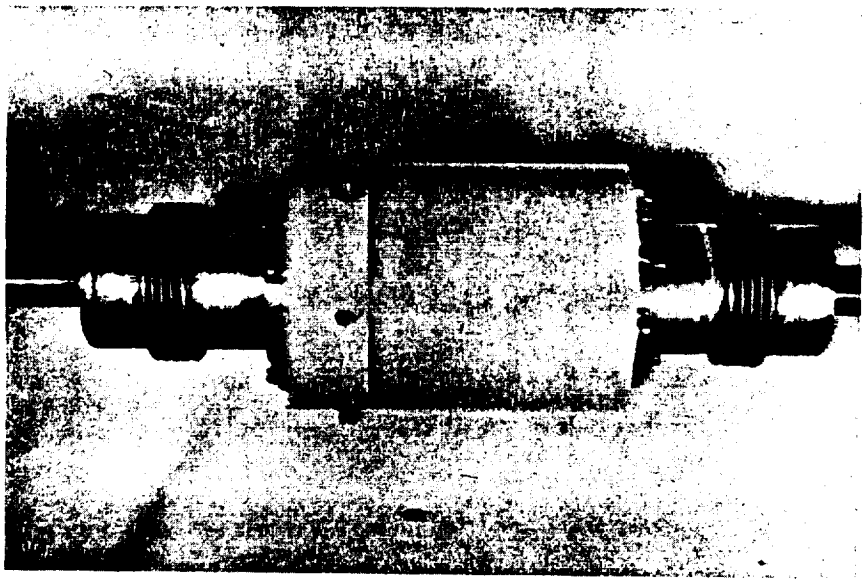

(A2b) Flowmeter installed in liquid nitrogen test circuit. Cylinders (with bellows) attached to the ends are vacuum jackets and are not part of the flowmeter.

Fig. A2 Electromagnetic flowmeter.

Appendix B

THE TRANSDUCER TUBE

The transducer tube is made up of four concentric cylinders of fiberglas (Panelyte 160) which are epoxied and bonded together to form a laminated tube. A detection electrode, a compensation electrode (a mirror image of the detection electrode and called detection electrode in this appendix), a driven-shield electrode, a symmetric ground electrode (a mirror image of the driven-shield electrode and called driven-shield electrode in this appendix), and a ground electrode are placed between the various cylinders as shown in Fig. B1. On each side of the transducer tube the innermost conductor of the triax connector is connected to a detection (or compensation) electrode and the intermediate conductor is connected to a driven-shield (or symmetric ground) electrode. A wire connected to the ground electrode is brought out through the end of the tube and is grounded to the flowmeter housing. The outer conductor of each triax connector is embedded in the outer fiberglas cylinder and is also grounded to the flowmeter housing.

The transducer electrodes are grids that are photoetched on both sides of copper-clad dielectric sheets (Mylar or teflon). The photoetch process allows one to create approximately 100 parallel conductors per inch on both sides of the dielectric sheet. These conductors are approximately 0.006-inch wide and are spaced 0.004-inch apart; the conductors are displaced so that all gaps on one side are covered by conductors on the opposite side. Figure B2 illustrates the detection electrode design. The parallel conductors are connected at their midpoint by one heavier cross-conductor.

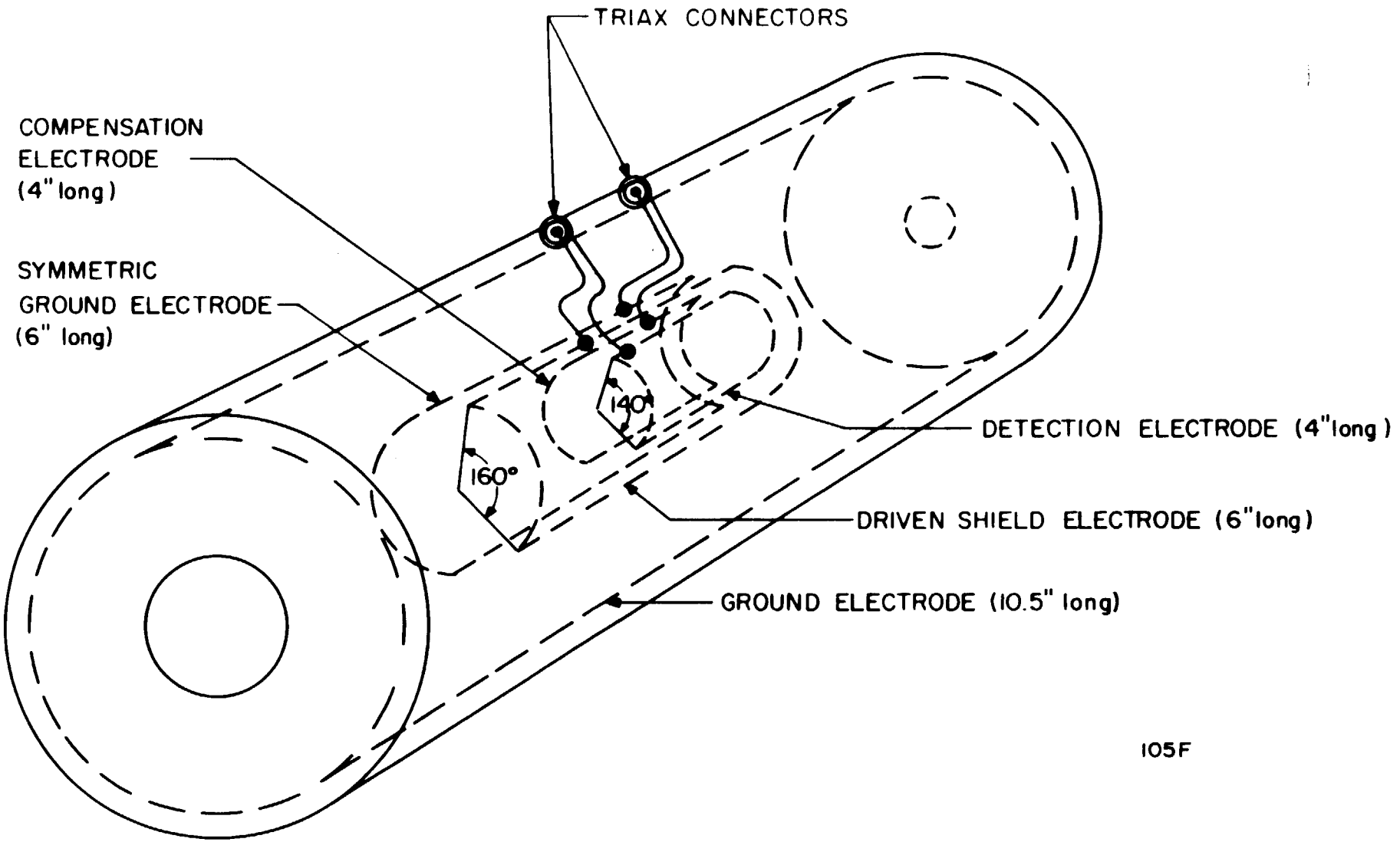

Fig. B1 Transducer electrode configuration. The compensation electrode and the symmetric ground electrode are mirror images respectively of the detection electrode and driven-shield electrode. The connections between the electrodes and the triax connectors are also shown.

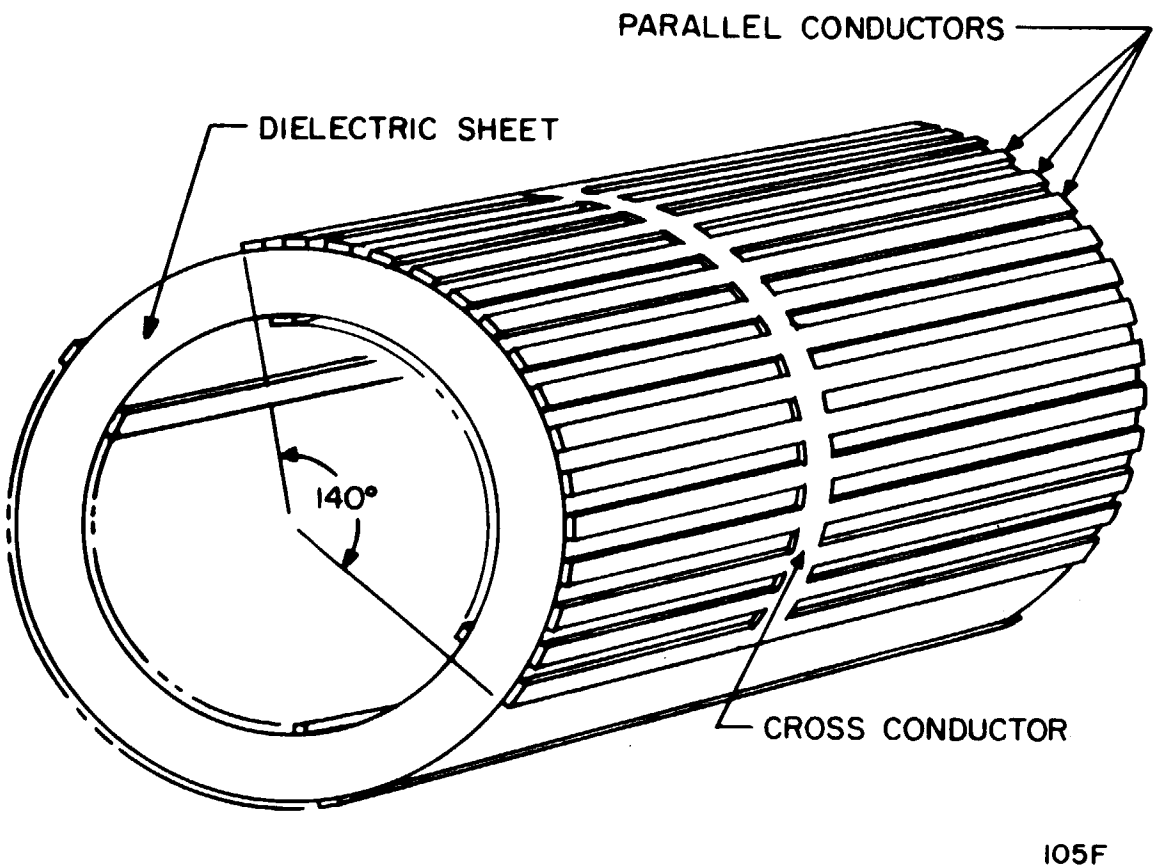

Fig. B2 The detection electrode grid. This drawing does not show actual proportions.

Several electrode fabrication methods were used before the photoetch method was adopted. Each method takes into account the basic design requirement for an electrode structure of wide area which does not provide an electrically conducting path for eddy currents. Such eddy currents would attenuate the magnetic field coupling the flowing fluid and thereby result in a reduced output signal from the transducer.

All of the designs consist of a grid of fine conductors (each conductor not closing on itself). In the final design these conductors run parallel to the axis of the transducer. Another method of electrode fabrication is to wrap one layer of fine wire (0.005-inch diameter or less) on the transducer tube (in a manner similar to wrapping thread on a spool) and cementing it in place. Unwanted conductor area is then machined away allowing the electrode conductor area to remain. All of these conductors are then connected together with a single wire which is in turn attached to the triax connector embedded in the transducer tube.

Still another fabrication method is to vacuum vapor deposit the grids on to the transducer tube. A rather costly masking screen is required when using this technique.

Table B-1 summarizes the characteristics of the various fabrication techniques in relation to ease of manufacture and ultimate quality.

TABLE B-I

TYPES OF ELECTRODE FABRICATION

Fabrication Method	Remarks
Wire Wrap	Wire diameters smaller than 0.005 in.; difficult to wind; connections relatively easy to make; fabrication time consuming; mechanically not as fragile as vapor deposited electrode.
Vapor Deposit	Fine conductors possible; difficult to make connections; fabrication difficult; mechanically fragile.
Photoetched (method adopted)	Conductors less than 0.006 in. wide difficult to make; connections easy to make; easy to fabricate; good mechanical strength.

The detection electrodes are 4 inches long; when applied to the transducer tube they subtend an angle of 140° on each side of the tube. The driven-shield electrodes are 6 inches long and subtend an angle of 160° on each side of the tube. The ground electrode, which is grounded to the flowmeter housing, is 10.5 inches long and subtends an angle of approximately 359°. In early attempts to fabricate a transducer tube a step change in mutual capacitnace between the detection electrode and associated driven-shield electrode--indicating an electrical rupture--was often noted during cool-down. In subsequent tubes the electrodes were not epoxied to the fiberglas, but rather

the copper-clad Mylar electrodes were coated with a silicone grease prior to epoxying the fiberglas cylinders together. Thus the electrodes are essentially floating between adjacent concentric fiberglas cylinders which are cemented together in all regions not containing electrodes. After assembly of the transducer tube the interelectrode capacitance was measured with the results shown in Table B-II. Side A and Side B are arbitrary designations for the two sides of each transducer tube.

TABLE B-II

INTERELECTRODE CAPACITANCES AT AMBIENT TEMPERATURE

	Side A	Side B
Detection to driven-shield electrode	52 picofarads	58 picofarads
Driven-shield to ground electrode	138 picofarads	166 picofarads
Detection to ground electrode	40 picofarads	45 picofarads

This transducer tube was next immersed in liquid nitrogen and capacitances measured while the tube was at a low temperature. Capacitances while cold are shown in Table B-III.

TABLE B-III

INTERELECTRODE CAPACITANCES AT LOW TEMPERATURES

	Side A	Side B
Detection to driven-shield electrode	47 picofarads	52 picofarads
Driven-shield to ground electrode	122 picofarads	148 picofarads
Detection to ground electrode	36 picofarads	40 picofarads

It will be noted that the capacitances measured on Side A and those measured on Side B differ. The degree of variation appears to be consistent with the geometrical tolerances in the concentric fiberglas cylinders which make up the transducer tube. The change in capacitance with cool-down is the cause of the zero point drift observed during cool-down of the flowmeter.

After the transducer tube is mounted in the flowmeter assembly, an amorphous Kel-F liner having a wall thickness of 0.030 inch is slid into the tube and flared at each end. Kel-F is chemically inert in relation to almost all fluids and in particular is relatively impermeable to hydrogen. The transducer tube with the Kel-F liner has been used in liquid nitrogen and liquid hydrogen flow tests for many hours and shows no electrical or mechanical damage.

Appendix C

TRIAX CONNECTORS

I. INTRODUCTION

The transducer tube in the electromagnetic flowmeter is a fiberglas tube in which the detection electrodes, the driven-shield electrodes, and the ground electrode are embedded. This tube is thermally insulated from the remaining portions of the flowmeter by a vacuum. The ground electrode is connected by a screw and lug to the flowmeter housing. The detection electrodes and driven-shield electrodes are connected to the electronics of the flowmeter by leads which pass through the vacuum and through the magnet coil. These leads must provide a vacuum seal and must be electrically shielded. Additionally, it was deemed advisable for the leads to be plug-in units at the transducer tube. Experience with earlier models had shown that leads permanently attached to the transducer tube were easily broken during handling, thus rendering the tube useless. To meet these requirements a triax connector was developed at the Engineering-Physics Company.

In the triax connector three brass conductors are arranged triaxially and insulated one from the other by a rigid dielectric. The center conductor is a solid wire and connects to the detection circuit. The intermediate conductor is a tube surrounding the center conductor and is slit lengthwise to minimize currents due to the alternating magnetic induction. This conductor is connected to the driven-shield electrode. The outer conductor surrounds the intermediate conductor and is also slit lengthwise; it is connected to the ground electrode and grounded at the flowmeter housing. The conductors

are embedded in a rigid dielectric which makes a vacuum seal with the dielectric jacket surrounding the vacuum region.

After considerable development--in which the major problem concerned effecting a suitably high vacuum (less than one micron Hg), low temperature seal between an electrical conductor and an electrical insulator--workable triax connectors were obtained. The connectors were used in the flowmeter during test runs of considerable duration with LH_2.

II. THE TRIAX CONNECTOR CONFIGURATION

The triax connector configuration is shown in Fig. C1. Amphenol Subminax coaxial connectors are used at the top and bottom of the triax connector. The bottom connector mates with a male connector embedded in the transducer tube and the top connector provides a means of electrically disconnecting the flowmeter electronics from the transducer tube without breaking the vacuum seal. The outer conductor of the connector is surrounded by a 0.031-inch thick plastic housing. A demountable vacuum seal is effected by an O-ring seal between the triax connector housing and a dielectric sleeve surrounding the connector. The connector housing and the dielectric sleeve for the triax connector are Delrin (an Acetal resin produced by E. I. du Pont de Nemours and Co.). This sleeve is screwed into the vacuum jacket. The seal at the screw threads is effected by machining the threads to produce a hand tight fit and then applying epoxy to the threads before final assembly. Once the epoxy is cured, the threaded sleeve is not removed.

The dielectric material separating the three concentric conductors is an epoxy, Hysol resin 4183 with hardener 3485. A vacuum seal within the

connector is obtained by breaking the coaxial configuration of the two inner conductors with a Delrin wall through which two small holes are drilled. These holes permit the center conductor and a wire from the intermediate conductor to pass from the vacuum region to the pressurized region. Hole clearance around the wires is about 0.001 inch. With this small area to seal, and using small diameter wires (0.019 inch) a vacuum seal can be made which is effective over a wide temperature range.

III. PREVIOUS TRIAX CONNECTOR DESIGNS

The initial design of a removable triax connector is shown in Fig. C2. The connector was similar to the final design with the following exceptions. The connector housing was sealed to the vacuum jacket with a face seal, and the vacuum seal within the connector was achieved by using epoxy between the conductors and their insulation. The end of the triax connector leading to the electronics terminated in several solder type leads rather than in a coaxial connector. Figure C2 shows the face seal on the Delrin vacuum jacket.

The above design had several shortcomings; the most noticeable was difficulty in mating the connector to the transducer tube and seating the face seal at the vacuum jacket simultaneously. This was overcome by the design shown in Fig. C3. The face seal was retained but was incorporated on the end of a separate sleeve. An O-ring on the connector body seals with the sleeve.

Fig. C4 shows the Delrin vacuum jacket. The jacket is wrapped with a ground shield; the wire shield has been removed where the connector face seals seat.

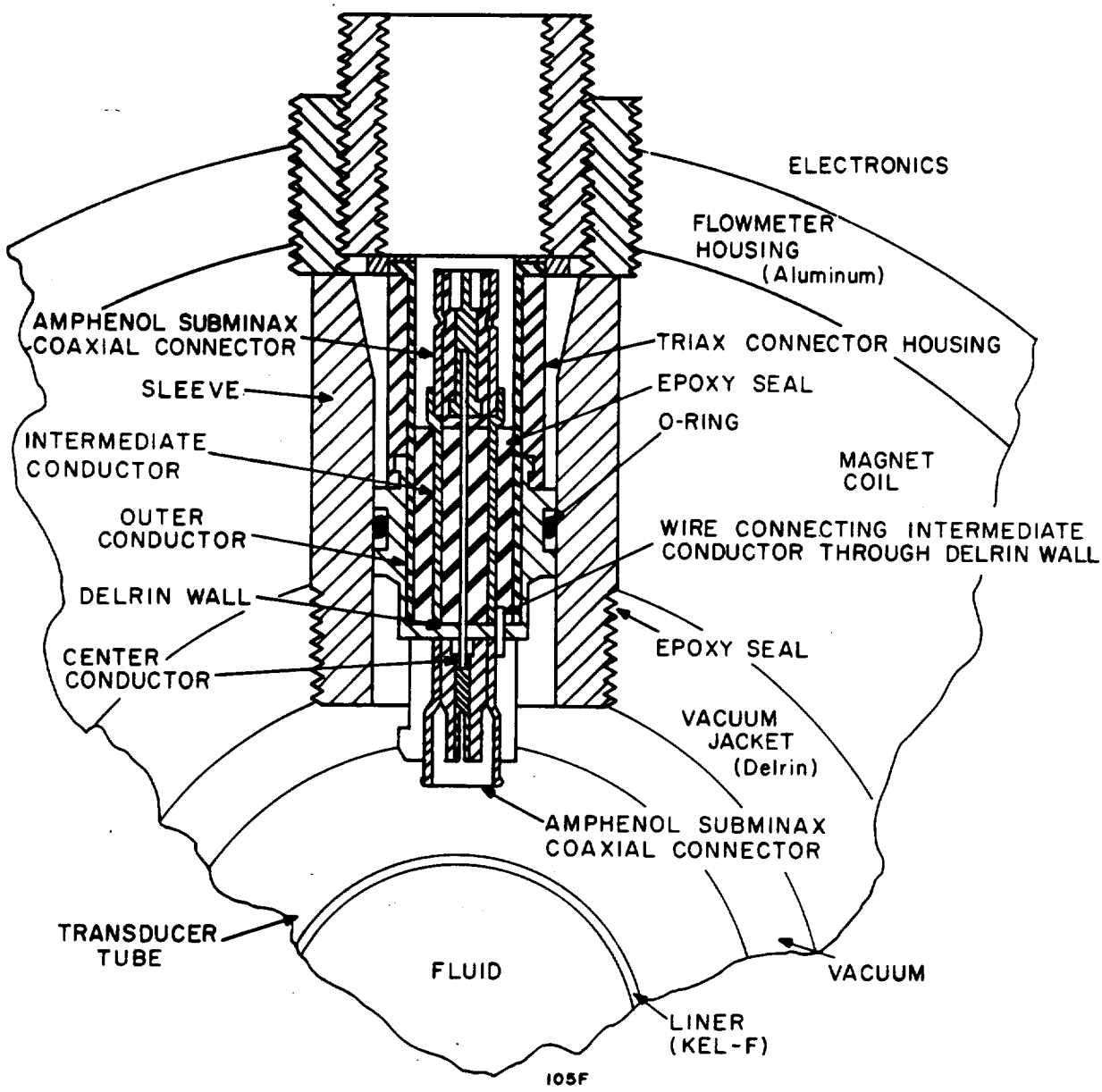

Fig. C1 The final triax connector design.

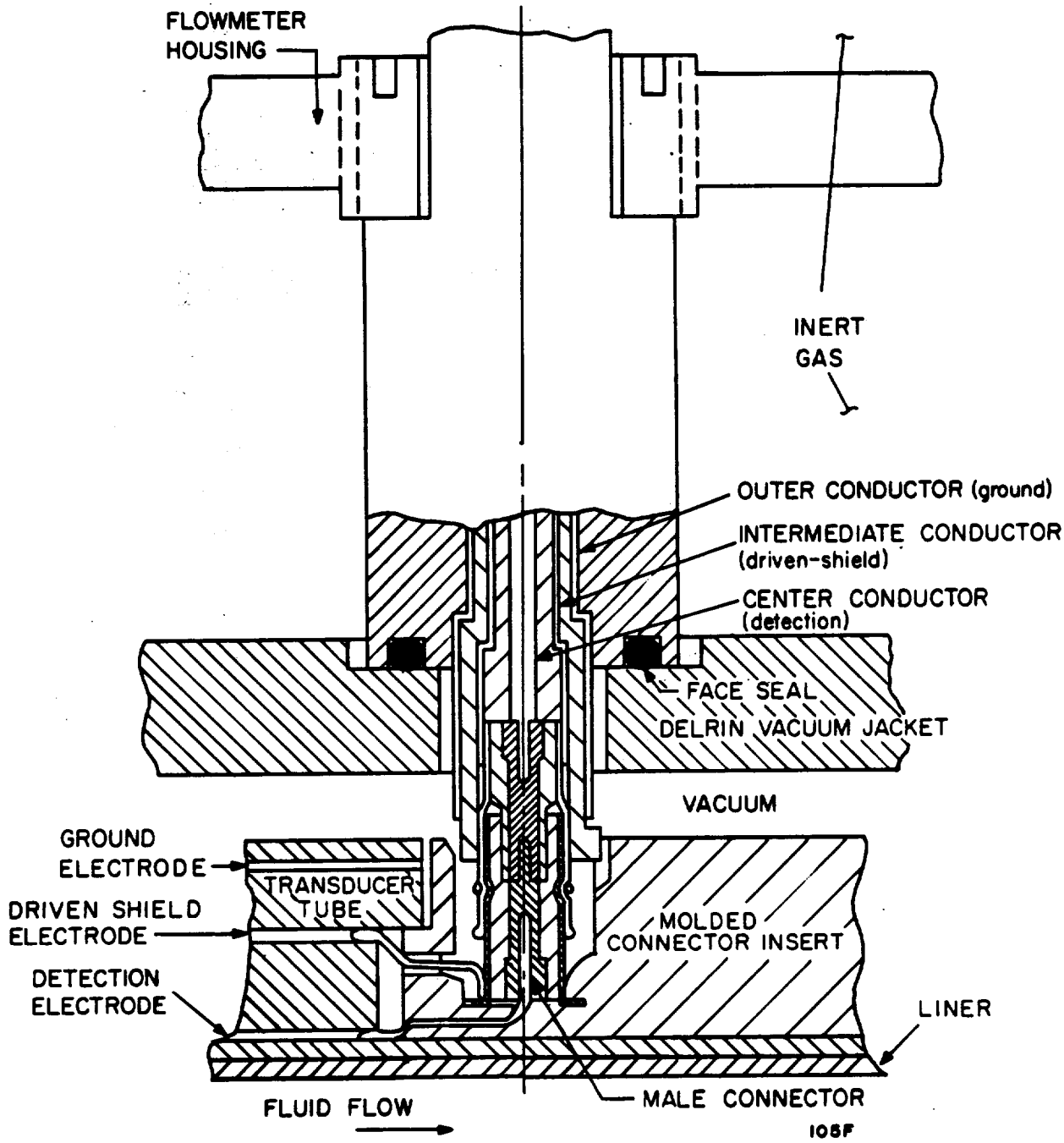

Fig. C2 The initial triax connector design.

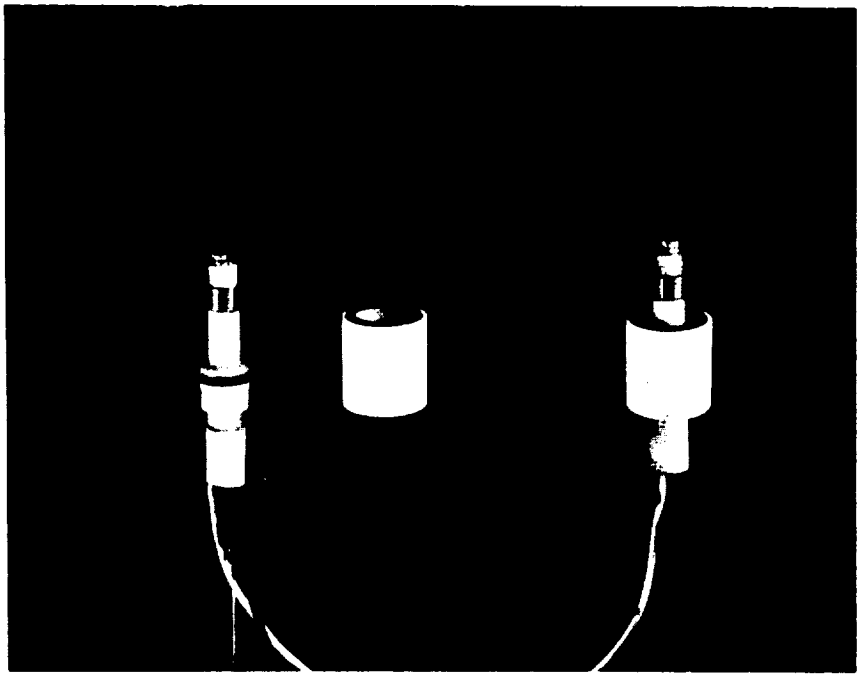

Fig. C3 Intermediate triax connector design. At the left is the connector; at the center is the separable sleeve with the connector; at the right is the assembled connector and sleeve.

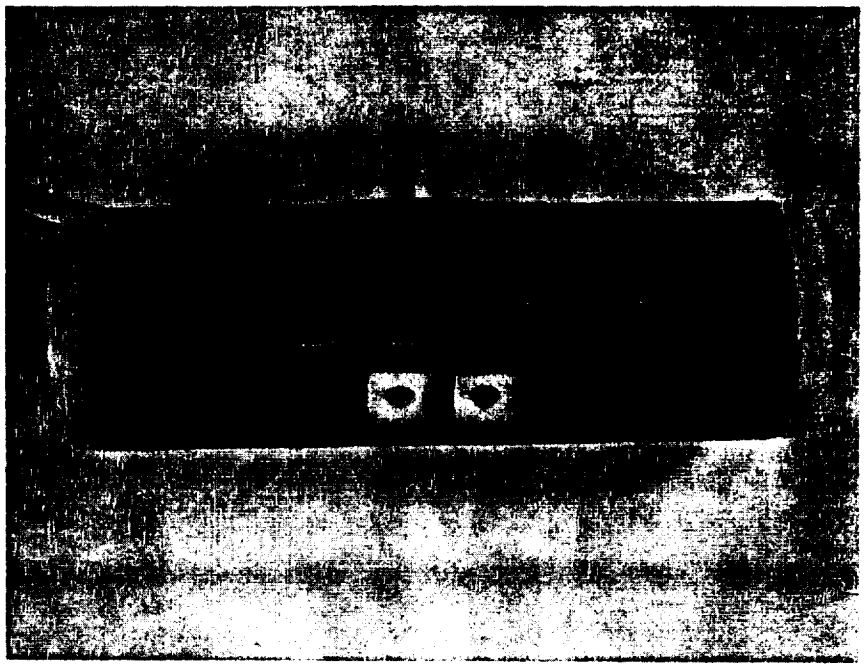

Fig. C4 Delrin vacuum jacket. A wire wound ground shield and the reference loop are attached to this component.

To eliminate the need for soldering the connector to the electronics section whenever it was desired to make or break this connection, an Amphenol coaxial connector was inserted at the top (pressurized end) of the triax connector. The triax connector was now beginning to look like the final design, but leaks were still occurring at the face seal. The problem was eliminated by screwing the sleeve into the Delrin vacuum jacket and epoxying the sleeve and jacket together to form a seal. This is shown in Fig. C1.

Leakage still continued within the connector along the interfaces between the conductors and their insulators. This problem was eliminated by feeding small diameter (0.019 inch) wires through small clearance (0.001 inch) holes in a Delrin wall and sealing with epoxy.

Appendix D

SEALS AND LINERS

I. GENERAL DESIGN

The electromagnetic flowmeter requires a nonmetallic transducer tube which will be impermeable to liquid hydrogen, will have a sufficiently high modulus of elasticity to be insensitive to pressure, and will permit connection to the system plumbing. The liner must be nonmetallic in order that the high frequency magnetic field through the fluid will not be attenuated. To obtain the combination of properties described above, the transducer tube is constructed with a high modulus of elasticity fiberglas for strength, and with a chemically inert liner gripped in flanges to provide the impermeability and sealing required.

The effectiveness of the liner impermeability and of the flanged seal was evaluated by inserting the transducer tube and liner into a cryogenic fluid line and then effecting a vacuum around the transducer tube. The degree of vacuum which could be maintained was an effective means of ascertaining the degree to which the liner contained the fluid. A very extended engineering investigation was carried out--first with teflon, and finally with Kel-F--before a successful arrangement was devised. The final design was successful in repeatedly containing a fluid flow of 100 gpm of both LN_2 and LH_2 through a liner 1-3/8 inches in diameter while a vacuum of less than 1 micron of mercury was maintained in an annular space surrounding the transducer tube.

The details of the liner and flange design are shown in Fig. D1. The liner material used here is 0.032-inch thick Kel-F-81 tubing, quenched as extruded to make it amorphous. The liner is terminated in a conical

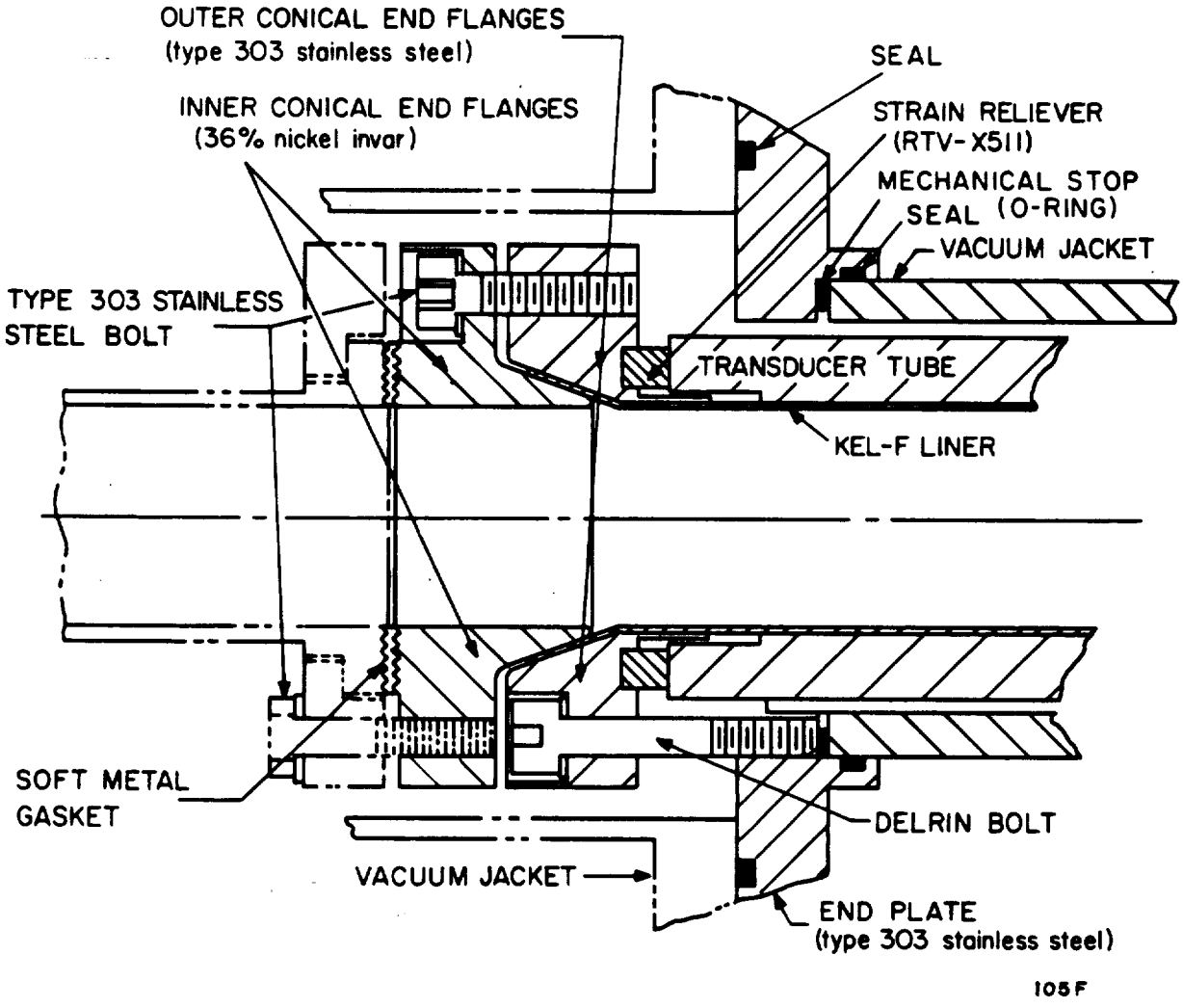

Fig. D1 Kel-F liner flange termination for liquid hydrogen.

(20 degrees) flare compressed between mating conical flange surfaces. The material of the outer flange is type 303 stainless steel, while the material of the inner flange is a 36 percent nickel Invar. The flowmeter attaches to the system plumbing with a soft metal gasket* compressed by a serrated profile formed by concentric rings. A molded ring made of General Electric RTV-X511 (a room temperature vulcanizing rubber for use at low temperatures) is placed between the stainless steel outer flange and the transducer tube to act as a strain reliever during cool-down.

II. DEVELOPMENT OF LINER AND SEAL

The transducer tube liner consists of a long cylindrical tube with the ends flared to form a gasket seal surface at the ends of the transducer tube. The first material considered was teflon because of its widely publicized chemical inertness and because it was known to stay elastic at temperatures well below that of LN_2.

An arrangement similar to that shown in Fig. D2 was used to test various types of flange seals. The teflon liner in this case was flared perpendicular to the axis of the tube.** The teflon was clamped between two

---

*The metal gaskets originally used by investigators at Lewis Research Center were lead, but they have since found the 1/32-inch-thick soft aluminum gaskets are even more reliable.

**The 90-degree flare was later eliminated in favor of a 20-degree conical flare.

metal flanges, one containing a raised 180° bead. A pipe thread connection was used to connect the inner volume to a vacuum system. After evacuating the inner volume, the assembly was dipped in LN_2 to a level above the flange seal but below the pipe connection. The effectiveness of the seal was evaluated by monitoring the vacuum during and after cool-down. In the case of the beaded flange, it was found that the teflon was deformed to such an extent by the bead that the flange would not hold a vacuum even at room temperatures.

Reduction of the unit loading on the teflon was attempted by replacing the metal bead with a neoprene O-ring as shown in Figs. D2b and D2c. In Fig. D2b the O-ring is behind the liner to prevent exposure to the fluid, and in Fig. D2c the O-ring is in direct contact with the fluid. Both types of seals were adequate for maintaining a vacuum while immersed in LN_2, although more trouble was experienced with the seal shown in Fig. D2b. The problem lay in the difficulty in containing the O-ring. If it is compressed unevenly it will not seal, and in one instance it pushed in the liner wall. In Fig. D2c the O-ring is effectively contained by metal and therefore uneven loading of the O-ring is not too likely to occur.

In a fourth type of flange seal, shown in Fig. D2d, the flared liner is compressed between two flat flanges. The unit pressure is lower but a very high bolt load is required to form a seal across the entire flange face. This seal was successfully tested in LN_2 on several occasions but was not always reliable, probably due to some variation or imperfection in the liner surface. Even with the lower unit pressure on the teflon liner a permanent compression set and thinning of the liner was evident.

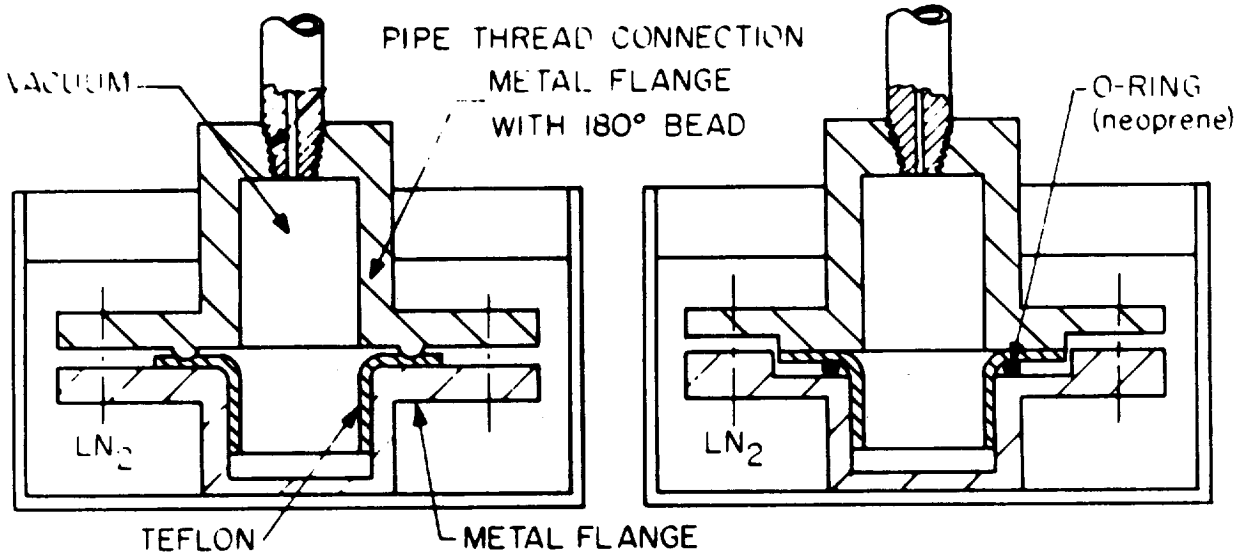

(a) 180° bead in metal flange.

(b) O-ring not exposed to fluid.

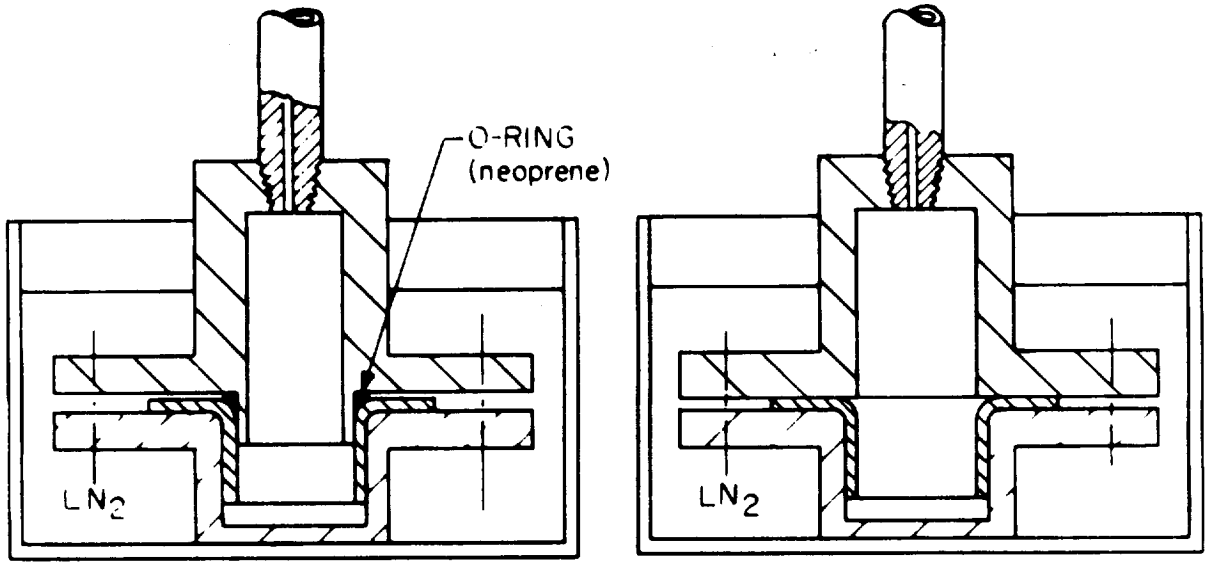

105F

(c) O-ring contained by metal flange (in contact with fluid).

(d) Flat surface contact with flanges.

Fig. D2 Flange seal test set-up.

Complete liner assemblies were constructed having a long tube (12 inches) with each end flared perpendicular to the axis and positioned over the inside diameter of a fiberglas tube. The seal was the type shown in Fig. D2d. When LN_2 was admitted inside the liner, failure (generally complete rupture or tearing) consistently occurred either on the first or second cool-down. All teflon liner failures occurred at the flared end section. Some liners were extremely distorted in the flared section which prevented maintaining a cryogenic seal, while other liners completely sheared at the end section. Two of these failures are shown in the photograph of Fig. D3.

Since all these failures occurred in the teflon which was exposed to the necessarily high temperature for flaring, a liner was machined to the same configuration and tested. This liner also failed in the same way, indicating that the weakness of this type of liner is probably inherent in the teflon and is not caused by the heat of flaring. Figure D4 shows the "clean" break of the machine flared end section from the liner.

A decrease of the stress at the liner flare was attempted by bonding the liner to the inside diameter of the fiberglas tube. Straight test sections (no flares) about four inches long were prepared and immersed in LN_2. The teflon shrank with respect to the fiberglas despite the epoxy bond. Because of the obvious bond failure, this approach was not pursued further.

The possibility of leaving the liner out and using the fiberglas pipe directly in contact with the fluid was considered. Inquiries relating to this approach were made and it was learned that the Materials Laboratory at NASA's Lewis Research Center had found fiberglas excessively porous to

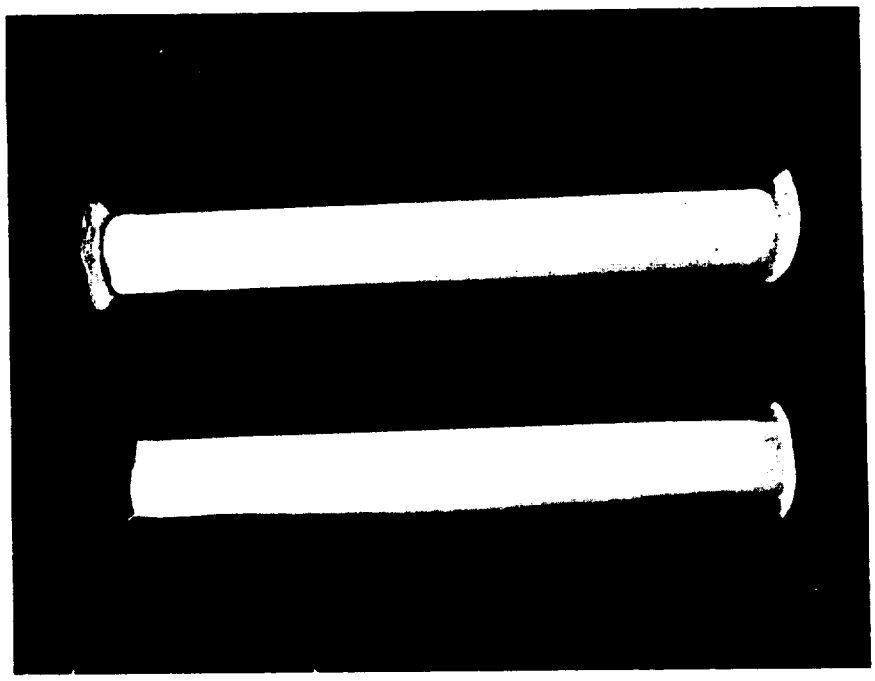

Fig. D3 Teflon liners after failure in liquid nitrogen test circuit.

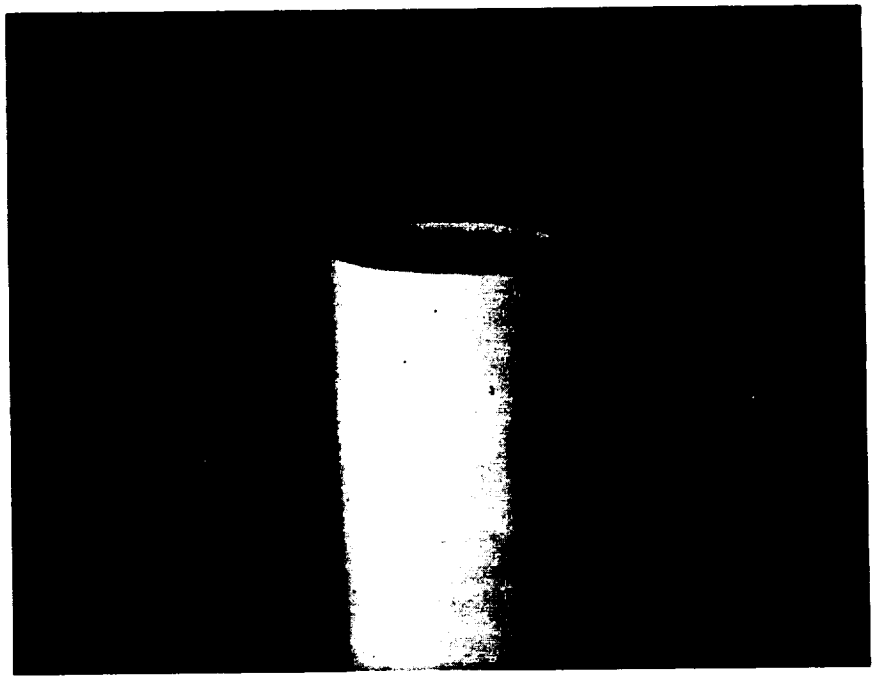

Fig. D4 Machined teflon liner after testing in liquid nitrogen. The flared section was completely sheared from this end.

hydrogen to the extent that it would not hold pressure. No further efforts were made along this line.

The liner material which was finally used is Kel-F-81 plastic flared at the ends to form 20-degree cones. The Kel-F is a fluorocarbon resin. In many respects it exhibits outstanding chemical resistance, but it also possesses a higher degree of toughness than teflon. The thermal contraction (between room temperature and LN_2 temperature) of Kel-F is approximately one-half that of teflon. Table D-I shows the comparative thermal contractions between 70°F and -320°F for Kel-F, teflon, and other selected materials. Although other materials have a lower coefficient of expansion, Kel-F was selected because it is easier to fabricate liners from Kel-F than, for instance, Mylar.

At first Kel-F liners and fiberglas tube assemblies were prepared with the liner flared to 90 degrees. These were repeatedly tested successfully in LN_2. Figure D5 shows one end of a flared Kel-F liner after several successful cycles between room temperature and LN_2 temperature.

However, when the Kel-F liner, which had been so successfully tested in LN_2, was subjected to LH_2, failure occurred almost immediately upon contact with the fluid. The failure was the type previously observed with the teflon liners, that is, one end sheared off near the 90 degree flare. Since tests had shown that the Kel-F liners would withstand temperatures down to -320°F but not to -423°F, it appeared that the liner could be made workable if the strain imposed by the additional 103°F were relieved. To accomplish this, strain relievers, the rectangular shaped silicone rubber rings shown in Fig. D1, were incorporated between the outer flange and the transducer tube. The material

TABLE D-I

THERMAL CONTRACTIONS OF SELECTED MATERIALS BETWEEN 70°F AND -320°F*

Material	Change of length per unit length (in./in.)
Quartz	<-0.0001
Invar	-0.0004
Glass cloth epoxy	-0.0028
Mylar	-0.0036
Kel-F-81	-0.0105
Teflon TFE	-0.0185

*These comparative values are taken from unpublished data compiled by the Materials Test Laboratory at NASA's Lewis Research Center. The data has been obtained on an informal basis and hence is subject to change. The information is reported here as the best available basis for EPCO's current work. The reader is cautioned to verify this data directly with Lewis Research Center before using it as a basis for further work.

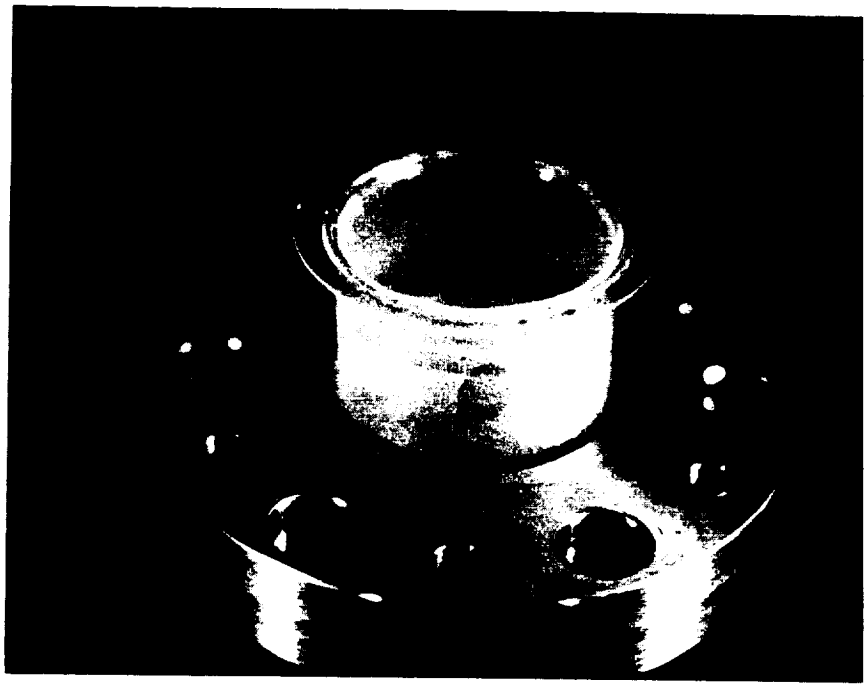

Fig. D5 End view of Kel-F test liner after several tests in liquid nitrogen with no apparent damage.

used is General Electric RTV-X511, a room temperature vulcanizing rubber, which remains flexible below -150°F. Initial strain in the liner is relieved by compression of the rubber. As the rubber starts to get cold, its thermal contraction will further relieve the strain on the liner. Although information is not available concerning the low temperature expansion coefficient of RTV-X511, the room temperature expansion coefficient of silicone rubbers is seventeen times as great as the room temperature expansion coefficient of Kel-F. Therefore, the thermal contraction of a relatively short length of the rubber will compensate for the thermal contraction of quite a long length of Kel-F.

To increase the unit loading on the liner flare, and to decrease the degree of bending of the flared section, the conical shaped seal (with a 20-degree flare) was designed (see Fig. D1). A higher sealing force is obtained because of the wedging action of the inner flange and because of the different coefficients of thermal contraction of the inner and outer flanges. The inner flange material is 36 percent nickel Invar and the outer flange material is 303 stainless steel. Invar has a coefficient of 1.1×10^{-6} in/in/°F between 0°F and -200°F. Stainless steel has a coefficient of thermal contraction of 7×10^{-6} in/in/°F over the same temperature range. The result therefore follows a self-energizing principle which was reported as being successfully used by S. E. Logan.*

*S. E. Logan, "Temperature-Energized Static Seal for Liquid Hydrogen," Advances in Cryogenic Engineering, Vol. 7, Paper L-9 (1961).

The physical properties of Kel-F depend upon its previous thermal history. It is common to speak of resins "quick-quenched" from their melting point of 414°F as amorphous, and of those "slow-cooled" as crystalline. At best these terms are relative since only suitably thin samples can be quenched rapidly and completely enough to inhibit crystal growth. The amorphous plastic is less dense, more elastic, and has a higher tensile strength, particularly at cryogenic temperatures, than the crystalline plastic.

For the above reasons the amorphous Kel-F is the most desirable for use at low temperatures. Although the plastic is purchased in the amorphous condition, flaring the ends to the 20-degree conical shape in the final design requires that the temperature at the end be raised almost to the melting point. It is very important that the plastic be quick-quenched immediately after flaring. Fig. D6 shows the arrangement used to flare the liner. Quenching is obtained by setting an appropriately shaped hollow aluminum container filled with cool water against the flared plastic. Immediately after the plastic has reached the desired shape, the hot tool is removed and the quick-quench tool is inserted. The flaring tool heat is provided by a 200 watt ring type heater attached to the back of the tool. Current is supplied to the heater through a variac. The temperature of the heater is maintained at the point where Kel-F will flare easily with a light hand pressure.

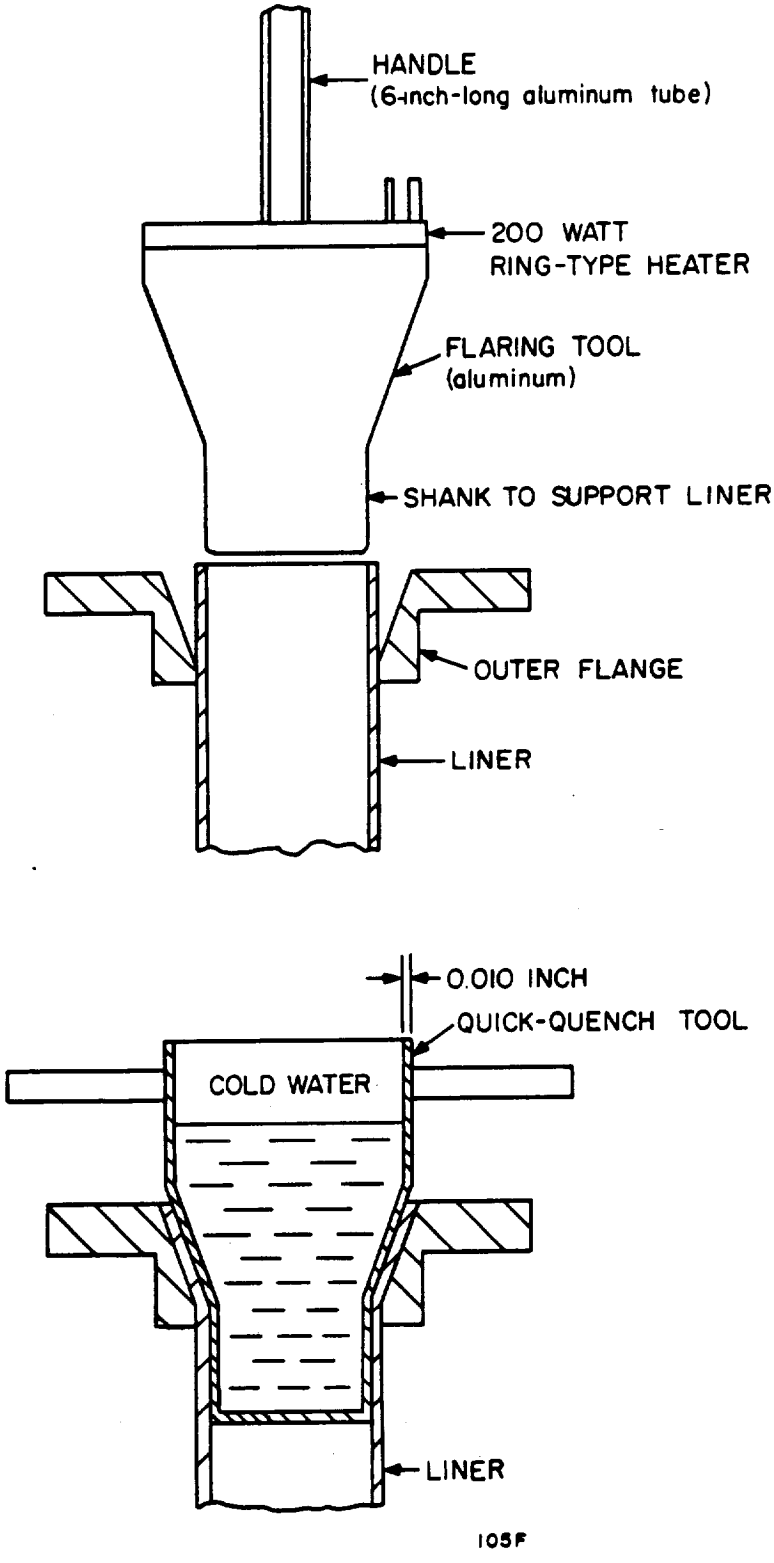

Fig. D6 Liner flaring tools.

Appendix E

MAGNET AND MAGNET POWER SUPPLY

I. INTRODUCTION

A uniform alternating magnetic field perpendicular to the direction of flow of the fluid is essential to the operation of the electromagnetic flowmeter. The system to be described here consists of (1) coil, (2) power amplifier, and (3) oscillator. Standard commercially available vacuum tube electronic packages are used here; however, should space and weight present a problem, a miniaturized, fully transistorized power supply is realizable.

The major design considerations taken into account in the selection of the present system were: amplitude and frequency stability, field strength, and cost. Since in the electromagnetic flowmeter the transducer voltage output is directly proportional to the flowrate and the flux density as well, it is essential that the magnetic field be of constant magnitude to maintain the calibration of the instrument. Additionally, since the electronic circuits used in the flowmeter are frequency sensitive, frequency stability is also required. The field strength was selected to give a usable signal level at the flowrates of interest.

II. MAGNET AND MAGNET CORE

Figure E1 shows the magnet. The uniformity of the field is established by winding the magnet coil such that the cross-section varies as a cosine function[1]. Litz wire is used to reduce the resistance increase due to skin

---

[1] V. J. Cushing and D. M. Reily, Final Report NASr-13.

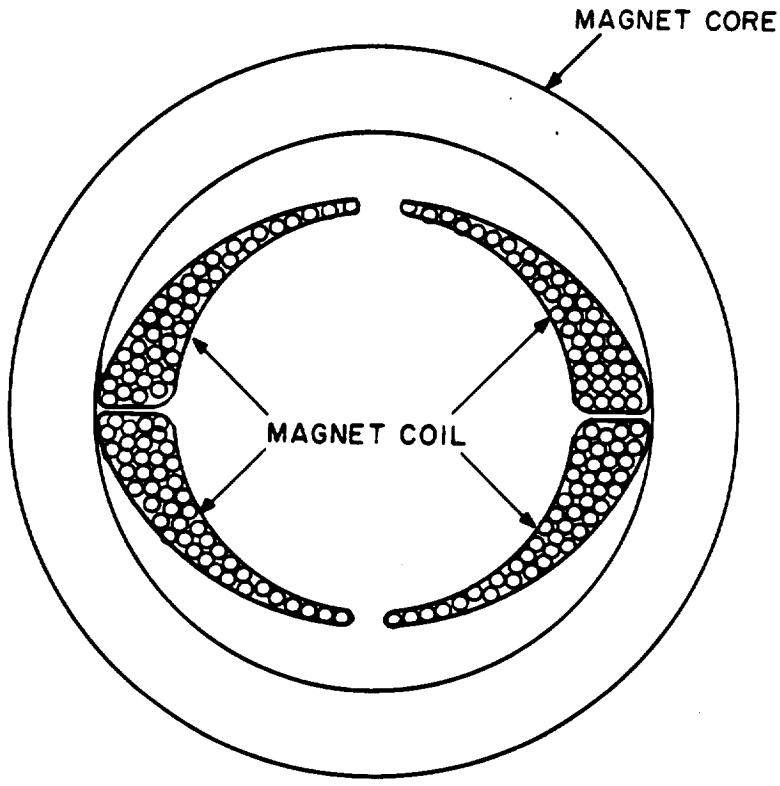

(a) CROSS SECTION

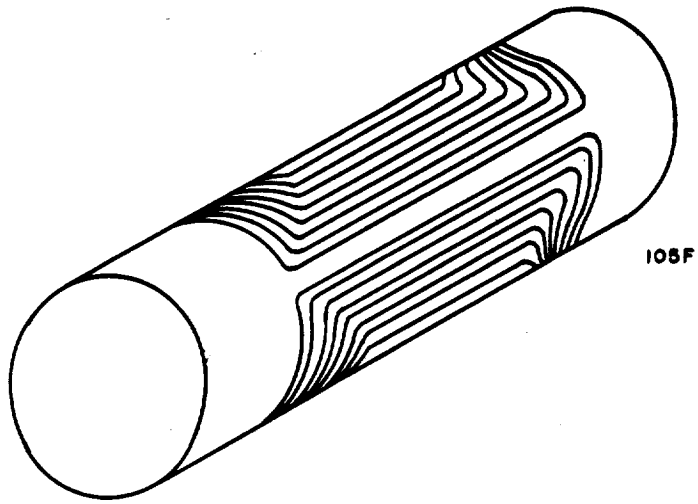

(b) SCHEMATIC OF MAGNETIC COIL

Fig. E1 The magnet coil and core.

effect. The coil Q increases as a direct result of the decreased coil resistance, bringing about a subsequent reduction in the required coil driving power. The coil is wound in two half-sections to simplify coil fabrication and to provide for easier assembly of the flowmeter. The coil is wound on a form with litz wire having a weave of 800 strands of No. 44 copper insulated with polythermalized enamel with an overwrap of two-ply nylon. The coil is coated with a silicone primer and then potted with a silicone rubber.

To reduce the reluctance of the magnetic path, toroidal powdered iron cores of Carbonal C[1] material were machined to fit the annular region between the outside of the coil and the flowmeter housing.

III. MAGNET POWER CIRCUIT

The magnet and magnet power supply circuit are shown in Fig. E2. The half-coils are connected in series and tuned with the necessary capacitance for resonance at 10 kc. The tuning capacitance consists of two capacitors[2] in series; the power amplifier[3] is connected across one of these capacitors in order to obtain a good impedance match. The input of the power amplifier is connected to a crystal oscillator[4] which supplies the 10 kc signal. When the amplifier is set to deliver maximum power the voltage measured from either coil end to ground is about 200 V rms. A linear relationship exists between the applied coil voltage and the flux density, hence indicating that there

---

[1] Arnold Engineering Co.

[2] Film Capacitors, Inc., A3-6-250.

[3] Scott Amplifier, Type 250-BRL.

[4] Bliley Oscillator, Type CCO-7RA-4

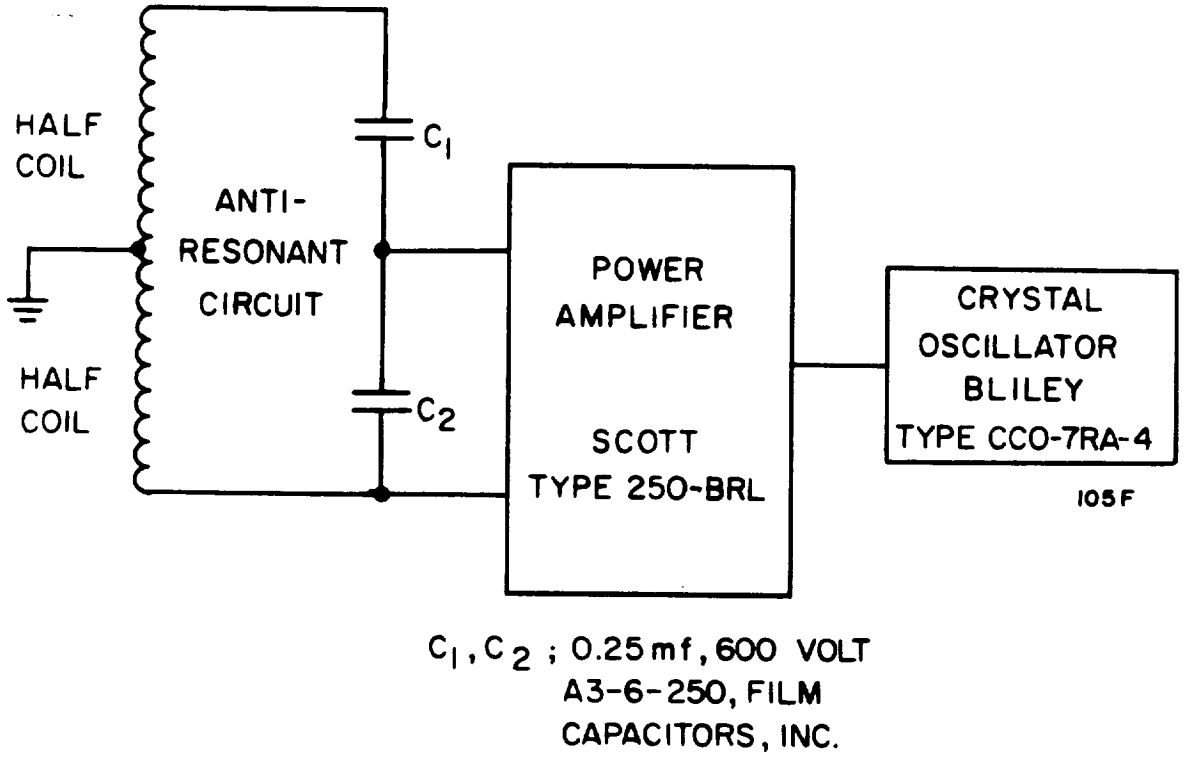

Fig. E2 Magnet and magnet power supply circuit.

are no saturation effects in the magnetic core material. The power amplifier and the oscillator are mounted in the control cabinet and a transmission line connects the power amplifier to the anti-resonant circuit in the flowmeter housing.

IV. EARLY MAGNET DEVELOPMENT

Prior to the final design the magnet coil had been driven indirectly by means of a set of secondary coils wound on the magnetic material of the flux return path. The initial reason for coupling in this fashion was to reduce the output impedance requirements of the power amplifier. In the final design, the secondary winding was eliminated and the matching of impedances was accomplished by splitting the tuning capacitance in the anti-resonant circuit as described earlier.

Various types of magnetic material had been tried before the Carbonal C* used in the final design was selected. Among those tried were magnetic tape. It was found, however, that special winding techniques were necessary in forming the magnetic return path and that only a thin cross-section was obtainable. Several epoxy-like magnetic materials were also tried; these were found to have too low a permeability and resulted in a low Q factor for the magnet coil.

---

*Arnold Engineering Company Carbonal C.

Appendix F

THE ELECTRONIC CIRCUIT

The electronic circuit for the electromagnetic flowmeter is used to amplify the flow signal from the transducer tube, and in turn processes the signal so as to extract the desired flowrate information. The electronic circuit is self-calibrating and can be controlled from a location remote from the flowmeter.

The signal produced by the transducer tube in the present design is about 1 millivolt. The signal source impedance is quite high, being primarily of the order of a 1 picofarad capacitive reactance. To amplify signals of this level and source impedance, a highly stabilized amplifier employing both negative and positive feedback was developed.

The signal obtained from the transducer tube contains voltage produced by the fluid flow and also the "transformer effect" voltage caused by the alternating magnetic field. In the present flowmeter, the "transformer effect" voltage or hum voltage is many times higher than the flow-produced voltage and must be nulled by means of a compensating voltage prior to amplification of the signal in order to prevent amplifier saturation. A compensation network was developed which provides for the injection of a compensation voltage at the transducer tube. Since the flow signal voltage is in quadrature with the hum voltage, the signal voltage is extracted from any residual hum voltage after amplification by means of a phase-sensitive voltmeter.

A calibration feature is also included so that the regenerative gain of the amplifier may be adjusted to the value required for operation in either the massmetric or volumetric mode. A block diagram of the flowmeter electronic circuit is shown in Fig. 3 in the main text. All of the electronics are in the control cabinet with the exception of the preamplifier. The flowmeter and the control cabinet are connected by means of a multi-circuit cable. A detailed schematic diagram of the electronic circuit is shown in Fig. F1 and a parts list follows.

In the remainder of this Appendix we describe the circuit development prior to arriving at the final configuration. The principal improvements effected were increased signal-to-noise ratio and increased amplifier stability.

Prior to arriving at the final design several of the amplifier stages had been direct coupled. It was decided to self-bias the amplifier stages wherever this had not been done and thereby facilitate checking of the noise level throughout each section of the electronic circuit.

The output amplifier, initially a cathode follower, was redesigned to provide for better stability by incorporating the output amplifier and the cathode follower formerly used to drive the outer conductor of the quadrax transmission line into a single compound feedback amplifier which serves both functions.

Decoupling networks were placed between input and second stage of the preamplifier, driven-shield amplifier, and output amplifier so as to minimize the possibility of interaction with low level stages.

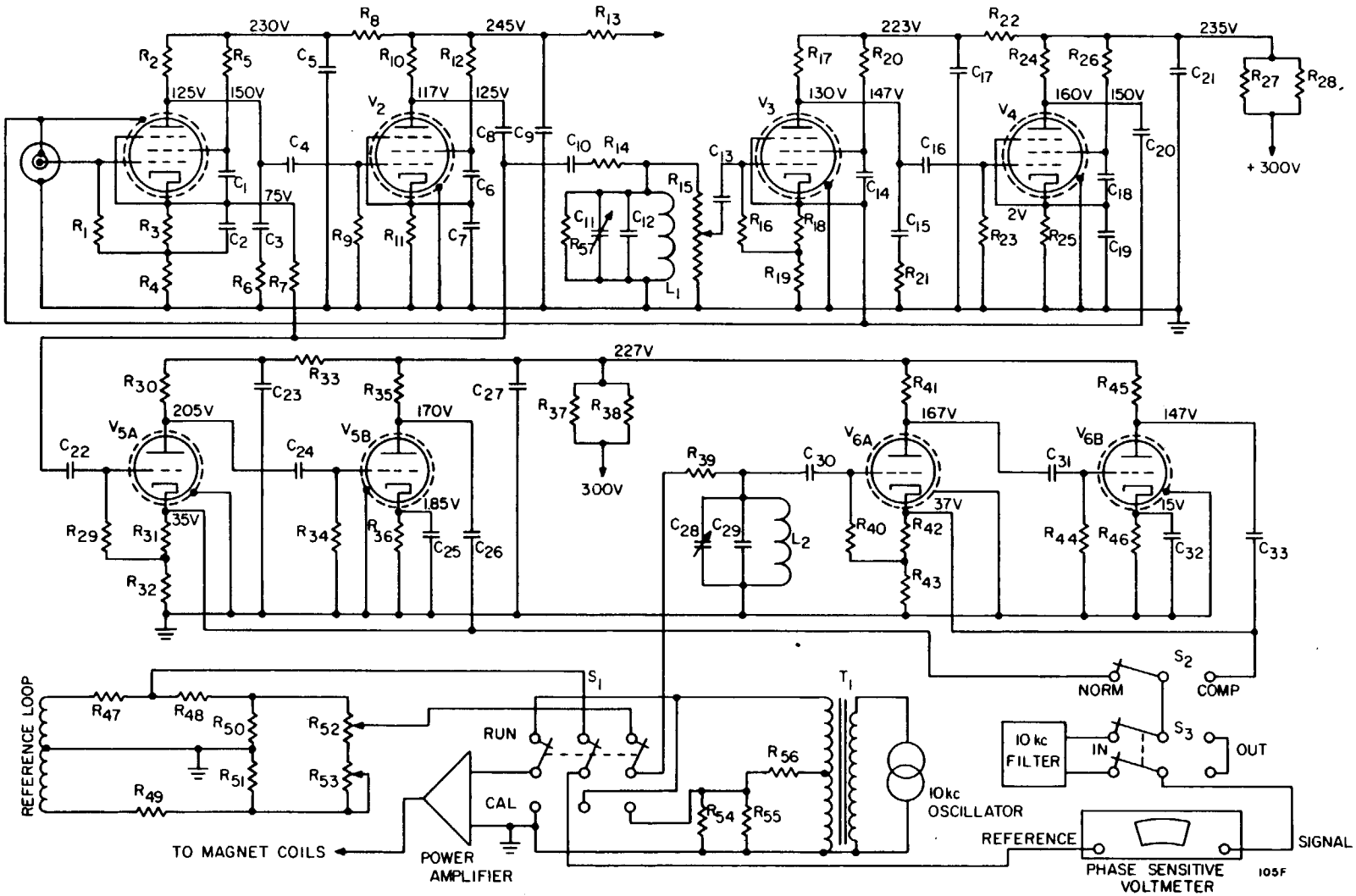

Fig. F1 Schematic diagram of the flowmeter electronic circuit.

PARTS LIST

Resistors

R_1	20 meg ± 5%	1/2 W	carbon composition
R_2	47 K ± 1%	1/3 W	wire wound
R_{31}, R_{18}	600 Ω ± 1%	1/3 W	wire wound
R_4, R_{38}, R_{43}	25 K ± 1%	1/3 W	wire wound
R_5	100 K ± 1%	1/3 W	wire wound
R_6, R_{21}	2.2 K ± 5%	1/2 W	carbon composition
R_7	2.0 K ± 1%	1/3 W	wire wound
R_8, R_{13}	4.7 K ± 1%	2.5 W	wire wound
R_9	270 K ± 10%	1/2 W	carbon composition
R_{10}, R_{24}	27.5 K ± 1%	2 W	wire wound
R_{11}, R_{25}	500 Ω ± 1%	1/3 W	wire wound
R_{12}	82 K ± 1%	1/3 W	wire wound
R_{14}	1 K ± 1%	1/3 W	wire wound
R_{15}	100 K potentiometer with vernier		wire wound
R_{16}, R_{44}	2.2 meg ± 5%	1/2 W	carbon composition
R_{17}, R_{45}	47 K ± 1%	1/3 W	wire wound
R_{19}	31.6 K ± 1%	1/2 W	deposited carbon
R_{20}	100 K ± 1%	1/2 W	deposited carbon
R_{22}	5 K ± 1%	1/3 W	wire wound
R_{23}	470 K ± 5%	1/2 W	carbon composition
R_{26}	82 K ± 1%	1 W	deposited carbon

PARTS LIST

Resistors, cont.

R_{27}, R_{28}, R_{37}	20 K ± 1%	1/3 W	wire wound
R_{29}	220 K ± 5%	1/2 W	carbon composition
R_{30}, R_{40}	10 K ± 1%	1/3 W	wire wound
R_{31}, R_{32}, R_{36}, R_{42}, R_{46}	1 K ± 5%	1/2 W	carbon composition
R_{33}, R_{49}	2 K ± 1%	1/3 W	wire wound
R_{34}	22 K ± 5%	1/2 W	carbon composition
R_{35}	30 K ± 1%	1/3 W	wire wound
R_{39}	5 K ± 1%	1/3 W	wire wound
R_{41}	40 K ± 1%	1/3 W	wire wound
R_{47}, R_{42}	1 K ± 1%	3 W	wire wound
R_{50}	100 Ω ± 1%	3 W	wire wound
R_{51}	100 Ω ± 1%	1/2 W	deposited carbon
R_{52}	2 K potentiometer with vernier		wire wound
R_{53}	100 Ω potientometer with vernier		wire wound
R_{54}, R_{55}	47 Ω ± 5%	1/2 W	carbon composition
R_{56}	12 K ± 5%	1/2 W	carbon composition
R_{57}	100 K ± 1%		wire wound

PARTS LIST

Capacitors

C_1, C_{14}	0.05 μf	400 V dc
C_2	50 μf	3 V dc
C_3, C_{15}	100 pf	600 V dc
C_4	0.04 μf	400 V dc
C_5, C_9, C_{17}, C_{21}, C_{23}, C_{27}	4 μf	350 V dc
C_6, C_{18}	1000 pf	1000 V dc
C_7	2 μf	150 V dc
C_8	0.1 μf	400 V dc
C_{10}	0.5 μf	100 V dc
C_{11}, C_{28}	3.5-100 pf variable air capacitors	
C_{12}, C_{29}	capacitance required to tune at 10 kc	
C_{13}	0.02 μf	100 V dc
C_{16}	220 pf NPO	1000 V dc
C_{19}, C_{32}	35 μf	3 V dc
C_{20}	0.22 μf	200 V dc
C_{22}	0.02 μf	400 V dc
C_{24}	0.05 μf	400 V dc
C_{25}	60 μf	6 V dc
C_{26}	0.1 μf	600 V dc
C_{30}	0.25 μf	100 V dc
C_{31}	0.005 μf	600 V dc
C_{33}	0.2 μf	400 V dc

PARTS LIST

Tubes

V_1, V_2, V_3, V_4	CK 5702	Raytheon
V_5 (A & B), V_6 (A & B)	6112	

Transformer

TI	5503 UTC

Inductors

L_1, L_2	150 mhy IV 1 kc UTC MQE-8

Oscillator

Bliley Type CCO-7RA-4

Power Amplifier

Scott Type 250-BRL

Power Supply

General Radio Model 1201-B

Sorensen Type QN/6.3 - 2.4

Phase-Sensitive Voltmeter

North Atlantic Model VN-204

A slightly different preamplifier design was tried prior to arriving at the final design. In an attempt to minimize the effects of tube and circuit noises as well as transmission pick-up noises it was decided to add an additional triode stage to the preamplifier circuit and additionally attain a voltage gain of approximately 10 from the latter two stages. This signal was then transmitted to the driven-shield amplifier. Hence, any noise voltages which would have been picked-up in the circuit in the second and third amplifier stages, in the driven-shield amplifier and along the transmission line would be effectively reduced by a factor of 10. It was found, however, that this change in configuration in itself did not bring about a gross change in the noise level of the overall circuit as had been anticipated; therefore it appeared that perhaps the largest amounts of noise might be coming from initial stages in the amplifier.

Since the circuits were being used primarily at rather low voltage levels the carbon composition resistors which were used in many of the low level quiescent current carrying amplifier circuits were generating noise due to resistance fluctuations commonly associated with the carbon composition resistor. A mathematical analysis of the noise levels expected as a result of such resistance fluctuation bore out the fact that a considerable amount of the observed noise was produced by this source. As a result, it was decided to replace all of the carbon composition resistors in quiescent current carrying circuits with non-inductive wirewound resistors. After replacing the carbon composition resistors with the wirewound resistors, approximately 12 db reduction in noise level was noted.

A further analysis of the circuit and circuit parameters indicated that the stability of the amplifiers could be considerably improved by redesign of the preamplifier and driven-shield amplifiers, and at this point it was decided to increase the degeneration and parlay the gain of 10 previously obtained so as to increase the stability of the preamplifier. One of the design criterion was to obtain as large a value of electrode voltage divided by electrode-to-cathode voltage as could be conveniently obtained without drastically altering the preamplifier configuration. A value of approximately 560 was obtained. After the design of the preamplifier had been completed a similar amplifier was designed for the driven-shield circuit. Upon the completion of these circuit designs each individual circuit, as well as the integrated circuit, was carefully checked for parasitic oscillations, and such circuits as were required to damp out these oscillations were included in the design.

In the original circuit with the Run-Off-Cal switch in the Cal position, the compensation voltage was shifted in phase approximately 45 degrees from the reference voltage. By moving a resistor (in series with the transformer on the oscillator output) to the other side of the Run-Off-Cal switch, this phase shift was eliminated. A change was also made in the resistors attached to the ends of the reference loop (on which the amplitude control operates). This change also improved the phase angle relationships within the circuits and the combination of changes appeared to markedly reduce the drift rate in the control circuit.

In the final design configuration a significant change in the magnitude of the hum voltage was noted when the compensation and symmetric ground cable connecting the transducer tube to the electronics was interchanged with the detection and driven-shield cable. As indicated in Appendix B on transducer design the cables should be interchangeable since the transducer electrodes are symmetrical. It is hypothesized that the change in the mechanical wiring configuration resulting from interchanging the cables caused a change in the transformer effect or hum voltage pick-up sufficient to cause the change in the magnitude observed.

Design data which assisted in the development of the final design, are given in Table FI. Using the available test points in the secondary and primary windings, measurements of hum under varying conditions were made. The numbers shown in the table indicate that lowered temperature does not cause an appreciable change in the phase angle of the hum, but does somewhat decrease the hum magnitude. The effect of removing the ground shield on the delrin vacuum jacket can be seen to be most important. The size of the interruption of the concentric cylinders within the triax connectors is also most vital if the outer ground shield is not connected. It is also of interest to note that removing the flowmeter cover changes the gain of the preamplifier but apparently does not effect the magnitude of the hum voltage generated within the flowmeter. Ungrounding the center of the secondary coils appears to give a minor reduction in the hum magnitude but this is certainly not a significant change.

TABLE FI

HUM MEASUREMENTS ON TRANSDUCER NO. 19

Read No.	Ground Shield	Triax Gap	Magn. Field	Meter Cover	Temp (^{o}K)	Flow	Measured Hum (mv)	Gain	Adj'd Hum (mv)	Phase Angle	Other Conditions
1	no	large	100%	on	80	35%	-1500	5	-300	3-1/2^{o}	
2	no	small	70%	off	amb.	0	- 265	3.26	- 81.4	2^{o}	
3	yes	small	70%	off	amb.	0	- 58	3.26	- 17.8	11^{o}	
4	yes	small	70%	on	amb.	0	- 53	2.98	- 17.8	7.5^{o}	
5	yes	small	70%	on	175	0	- 53	2.93	- 18.1	10^{o}	
6	yes	small	70%	on	99	0	- 53	3	- 17.6	10^{o}	
7	yes	small	70%	on	86	0	- 50	3	- 16.7	10^{o}	
8	yes	small	70%	on	79	0	- 42	2.58	- 16.3	10^{o}	
9	yes	small	70%	on	80	35%	- 45	3	- 15.0	8.5^{o}	
10	yes	small	70%	off	amb.	0	- 56	3.26	- 17.2	11^{o}	secondary floating
11	yes	small	70%	off	amb.	0	- 140	3.26	- 43	3.5^{o}	one side grounded
12	yes	small	70%	off	amb.	0	- 20	3.26	- 6.1	135^{o}	other side grounded

Appendix G

LN_2 FLOW TEST FACILITY

I. - INTRODUCTION

To satisfy routine cryogenic testing requirements for the development of the flowmeter, a LN_2 flow test circuit was constructed at the Engineering-Physics Company laboratory. This test circuit allowed the investigation of the mechanical as well as electrical performance of the flowmeter at cryogenic temperatures and permitted the solution of many basic problems before final tests in liquid hydrogen.

II. DESCRIPTION OF TEST CIRCUIT

The LN_2 flow test circuit at the Engineering-Physics Company has a regulated flowrate from a minimum of approximately 10 gpm to an estimated maximum flowrate of 160 gpm. The maximum flowrate must be estimated since the reference turbine meter has a full scale output corresponding to 110 gpm. The main portion of the flow circuitry is covered with solid insulation; but the flowmeter itself is insulated with vacuum (1.0 to 10.0 microns of Hg) insulation for application to LH_2. A cryogenic thermometer and Bourdon type pressure gages continuously monitor the fluid state.

The test circuit is shown schematically in Fig. G1 and photographically in Figs. G2 and G3. The LN_2 is stored in a 300 gallon liquid nitrogen dewar (Model VV 36-300-250 built by Hofman Laboratories, Hillside, New Jersey). The fluid is diven by a Turbocraft Series 3000 pump with a variable speed drive motor. The reference turbine meter is a Fischer and Porter Co. Turbine Meter Model 10C-1505. Most of the plumbing consists of copper tubing with sweat type fittings. The size of the tubing at different sections of the test

circuit is shown in Fig. G1. The test flowmeter is inserted in the middle of a 5-foot length of stainless steel tubing have an ID of 1.38 inches which is the same ID as the flowmeter. All manual in-flow valves are gate type valves to provide minimum flow obstruction. The manual vent valves are globe valves since obstruction to flow is not a consideration here and the cost of globe valves is less than that of gate valves.

The test facility is physically located such that the storage dewar, pump, and one safety valve are located outside of the laboratory; the remainder of the test circuit is located inside the laboratory. The safety valve connected to the plumbing inside the building is set to open at 100 psig. This safety valve vents outside the laboratory through a copper tube. The safety valve located outside is set to vent at 150 psig pressure. A 1/2-inch diameter globe valve located inside the laboratory permits the entire system to be pressurized from an external source. This has been extremely useful in hunting for leaks in the system.

Except for the vacuum insulation around the flowmeter itself, the entire plumbing is covered with solid insulation. This insulation consists of a layer of asbestos tape 1/16-inch thick by 3-inches wide wrapped spirally around the copper tubing. The asbestos protects the tubing from a 1-1/2-inch thick shell of foam glass which provides the next layer of insulation. Covering the foam glass is a 1-1/2-inch thick layer of fiberglas backed with an aluminum foil jacket. All seams in the foil are sealed with an aluminum paint. The insulation is clearly visible in Figs. G2 and G3.

For safety reasons, the portion of the test circuit outside the laboratory is enclosed with a 6-foot high chain link fence. Inside the

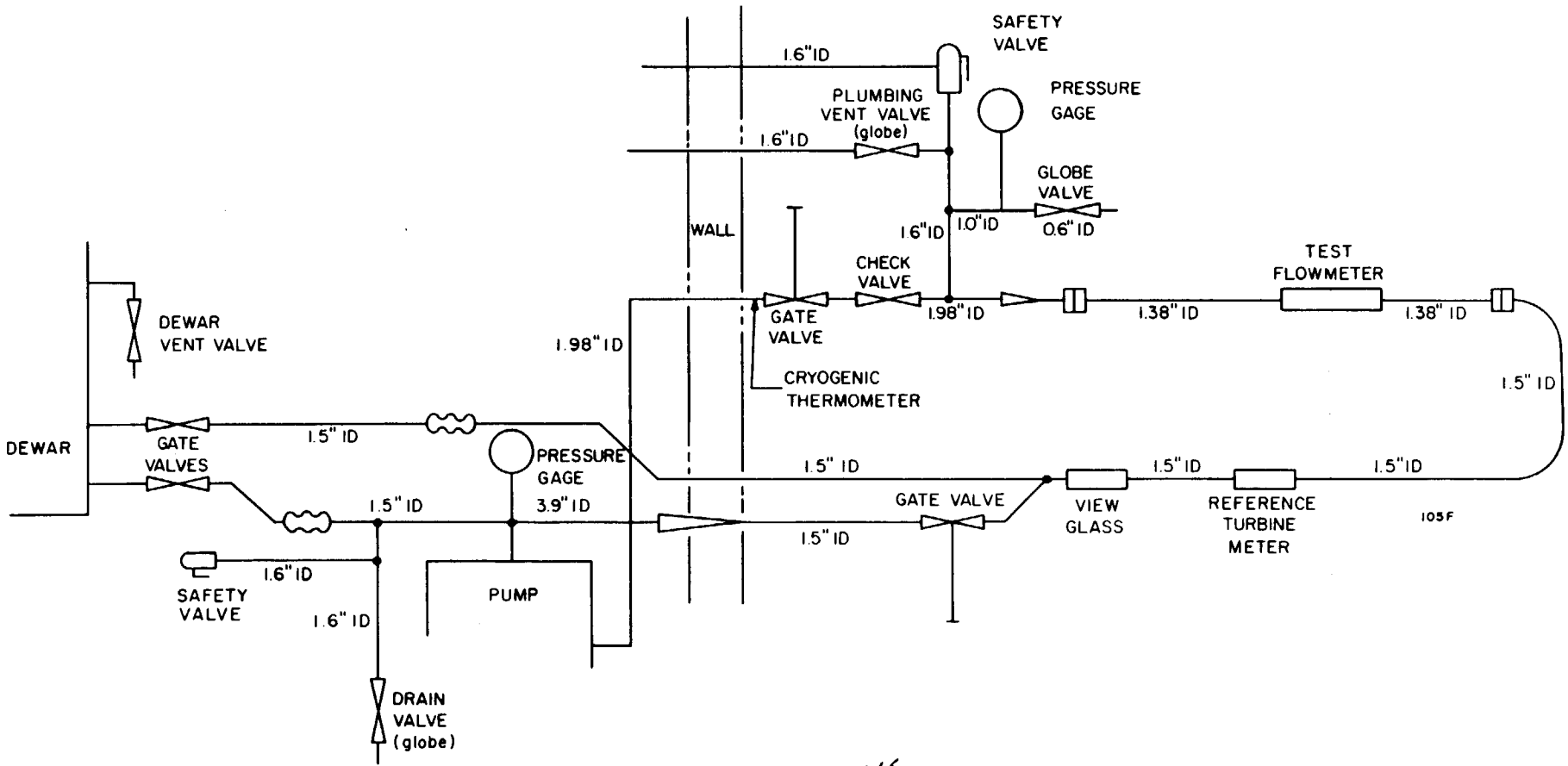

115

Fig. G1 Test installation.

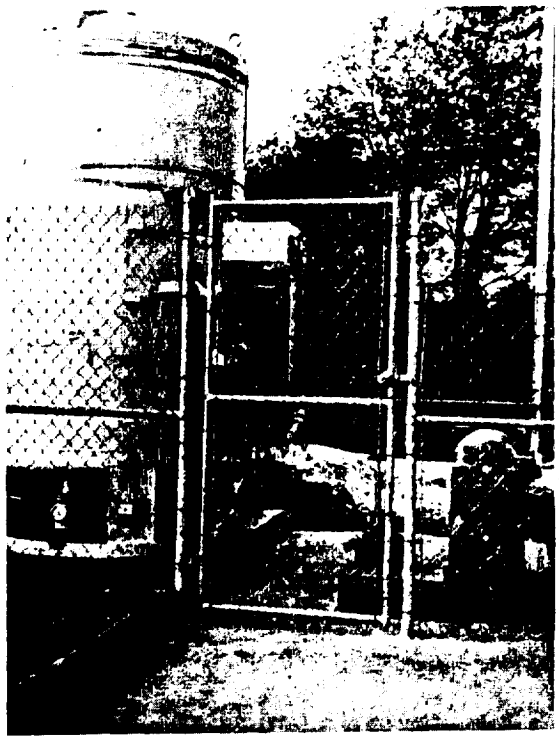

Fig. G2 Liquid nitrogen installation--storage tank and pump.

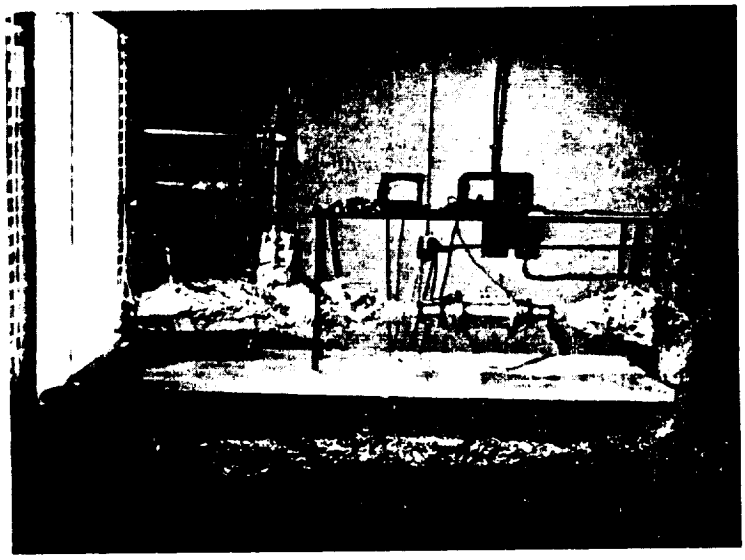

Fig. G3 Liquid nitrogen installation--test circuit.

laboratory there is useable bench space and a shelf for associated meters. Visible in Fig. G3 are the readout meters for the reference turbine meter and the vacuum gage.

III. OPERATION OF TEST CIRCUIT

During the operation of the test circuit, flow is out of the dewar and into the pump. The level of the fluid in the dewar is above the pump so that a positive head is maintained upon the pump intake at all times. Upon leaving the pump, the fluid is raised a distance of 3 feet, passes through a gate valve, a check valve, and then through the flowmeter, after which it drops a distance of 2 feet, passes through the reference turbine meter and approaches a branch in the plumbing. One section returns the fluid directly to the dewar while the other section returns the fluid to the intake side of the pump. The amount of fluid returning directly to the inlet of the pump is regulated by a 1-1/2-inch gate valve. This quick return to the pump is necessitated by the piping within the dewar which if used as the only return circuit would preclude obtaining more than 60 gpm of flow. Flowrate is controlled by pump speed, and by the degree to which the gate valves are opened.

To begin a test run the system is first cooled. This is accomplished by opening the dewar supply and return valves and by cracking the plumbing vent valve so that pressure will build up in the system to about 20 to 30 psig while cool-down occurs. The amount of pressurization is controlled either by the plumbing vent valve or by the dewar vent valve. When the

system nears LN_2 temperature the motor is turned on. A running condition is obtained when the two pressure gages on either side of the pump show a 10 to 12 psi pressure differential. It has been found that opening the plumbing vent valve and discharging fluid for about 2 seconds is helpful in promoting a running condition.

DISTRIBUTION LIST CONTINUED

COPIES	RECIPIENT	DESIGNEE
2	Marshall Space Flight Center Huntsville, Alabama 35812	Hermann K. Weidner Code M-P&VED
2	Manned Spacecraft Center Houston, Texas 77001	Robert R. Gilruth Director
1	Advanced Research Projects Agency Washington 25, D. C.	D. E. Mock
1	Aeronautical Systems Division Air Force Systems Command Wright-Patterson Air Force Base Dayton, Ohio	D. L. Schmidt Code ASRCNC-2
1	Air Force Missile Development Center Holloman Air Force Base, New Mexico	Maj. R. E. Bracken Code MDGRT
1	Air Force Missile Test Center Patrick Air Force Base, Florida	L. J. Ullian
1	Air Force Systems Command, Dyna-Soar Air Force Unit Post Office Los Angeles 45, California	Col. Clark Technical Data Center
1	Arnold Engineering Development Center Arnold Air Force Station Tullahoma, Tennessee	Dr. H. K. Doetsch
1	Bureau of Naval Weapons Department of the Navy Washington 25, D. C.	J. Kay, Code RTMS-41
1	Central Intelligence Agency 2430 E Street, N. W. Washington 25, D. C. Attn: Miss Elizabeth F. Kernan	
1	Defense Documentation Center Headquarters Cameron Station, Building 5 5010 Duke Street Alexandria, Virginia 22314 Attn: TISIA	
1	Headquarters, U. S. Air Force Washington 25, D. C.	Col. C. K. Strambaugh Code AFRST
1	Picatinny Arsenal Dover, New Jersey	I. Forsten, Chief Liquid Propulsion Laboratory

DISTRIBUTION LIST

COPIES	RECIPIENT	DESIGNEE
10	NASA Lewis Research Center 21000 Brookpark Road Cleveland, Ohio 44135 Contracting Officer, Chemical Rocket Systems Procurement	(X)
	NASA Headquarters, Washington, D. C. 20546	
4	Mr. Henry Burlage, Jr. Chief, Liquid Propulsion Systems, RPL	(X)
1	Mr. Vernon E. Jaramillo Advanced Manned Mission, MTA	(X)
25	Scientific and Technical Information Facility NASA Representative, Code CRT P. O. Box 5700 Bethesda, Maryland 20014	(X)

NASA FIELD CENTERS

COPIES	RECIPIENT	DESIGNEE
2	Ames Research Center Moffett Field, California 94035	Harold Hornby Mission Analysis Division
2	Goddard Space Flight Center Greenbelt, Maryland 20771	Merland L. Moseson Code 623
2	Jet Propulsion Laboratory California Institute of Technology 4800 Oak Grove Drive Pasadena, California 91103	Robert F. Rose Propulsion Div., 38
2	Langley Research Center Langley Station Hampton, Virginia 23365	Floyd L. Thompson Director
2	Lewis Research Center 21000 Brookpark Road Cleveland, Ohio 44135	Dr. Abe Silverstein Director

DISTRIBUTION LIST CONTINUED

COMMERCIAL CONTRACTORS

COPIES	RECIPIENT	DESIGNEE
1	Astropower, Inc., Subsidiary of Douglas Aircraft Company 2968 Randolph Avenue Costa Mesa, California	Dr. George Moc Director, Research
1	Astrosystems, Inc 1275 Bloomfield Avenue Caldwell Township, New Jersey	A. Mendenhall
1	Atlantic Research Corporation Edsall Road and Shirley Highway Alexandria, Virginia	A. Scurlock
1	Beech Aircraft Corporation Boulder Facility Box 631 Boulder, Colorada	J. H. Rodgers
1	Bell Aerosystems Company P. O. Box 1 Buffalo 5, New York	W. M. Smith
1	Bendix Systems Division Bendix Corporation Ann Arbor, Michigan	John M. Brueger
1	Boeing Company P. O. Box 3707 Seattle 24, Washington	J. D. Alexander
1	Chrysler Corporation Missile Division Warren, Michigan	John Gates
1	Curtiss-Wright Corporation Wright Aeronautical Division Wood-Ridge, New Jersey	G. Kelley
1	Douglas Aircraft Company, Inc. Missile and Space Systems Division 3000 Ocean Park Boulevard Santa Monica, California 90406	R. W. Hallet Chief Engineer Advanced Space Techniques
1	Fairchild Stratos Corporation Aircraft Missiles Division Hagerstown, Maryland	J. S. Kerr

DISTRIBUTION LIST CONTINUED

COPIES	RECIPIENT	DESIGNEE
1	Rocket Research Laboratories Edwards Air Force Base Edwards, California	Col. H. W. Norton
1	U. S. Atomic Energy Commission Technical Information Services Box 62 Oak Ridge, Tennessee	
1	U. S. Army Missile Command Redstone Arsenal, Alabama 35809	Dr. Walter Wharton
1	U. S. Naval Ordnance Test Station China Lake, California	E. Yim, Jr., Chief Missile Propulsion Division, Code 451
1	Chemical Propulsion Information Agency Johns Hopkins University Applied Physics Laboratory 8621 Georgia Avenue Silver Spring, Maryland	Neil Safeer

COMMERCIAL CONTRACTORS

COPIES	RECIPIENT	DESIGNEE
1	Aerojet-General Corporation P. O. Box 296 Azusa, California	L. F. Kohrs
1	Aerojet-General Corporation P. O. Box 1947 Technical Library, Bldg. 2015, Dept. 2410 Sacramento 9, California	R. Stiff
1	Aeronutronic A Division of Ford Motor Company Ford Road Newport Beach, California	D. A. Carrison
1	Aerospace Corporation 2400 East El Segundo Boulevard P. O. Box 95085 Los Angeles, California 90045	John G. Wilder MS-2293 Propulsion Dept.
1	Arthur D. Little, Inc. Acorn Park Cambridge 40, Massachusetts	A. C. Tobey

DISTRIBUTION LIST CONTINUED

COMMERCIAL CONTRACTORS

COPIES	RECIPIENT	DESIGNEE
1	Martin Denver Division Martin Marietta Corporation Denver, Colorado	J. D. Goodlette Mail A-241
1	McDonnell Aircraft Corporation P. O. Box 6101 Lambert Field, Missouri	R. A. Herzmark
1	North American Aviation, Inc. Space & Information Systems Division Downey, California	H. Storms
1	Northrop Corporation 1001 East Broadway Hawthorne, California	W. E. Gasich
1	Pratt & Whitney Aircraft Corp. Florida Research and Development Center P. O. Box 2691 West Palm Beach, Florida	R. J. Coar
1	Radio Corporation of America Astro-Electronics Division Defense Electronic Products Princeton, New Jersey	S. Fairweather
1	Reaction Motors Division Thiokol Chemical Corporation Denville, New Jersey 07832	Arthur Sherman
1	Republic Aviation Corporation Farmingdale, Long Island, New York	Dr. William O'Donnell
1	Rocketdyne (Library Dept. 586-306) Division of North American Aviation 6633 Canoga Avenue Canoga Park, California 91304	E. B. Monteath
1	Space General Corporation 9200 Flair Avenue El Monte, California	C. E. Roth
1	Space Technology Laboratories Subsidiary of Thompson-Ramo-Wooldrige P. O. Box 95001 Los Angeles 45, California	G. W. Elverum

DISTRIBUTION LIST CONTINUED

COMMERCIAL CONTRACTORS

COPIES	RECIPIENT	DESIGNEE
1	General Dynamics/Astronautics Library & Information Services (128-00) P. O. Box 1128 San Diego, California 92212	Frank Dore
1	General Electric Company Missile and Space Vehicle Department 3198 Chestnut Street, Box 8555 Philadelphia 1, Pennsylvania	L. S. Beers
1	General Electric Company Flight Propulsion Lab Department Cincinnati 15, Ohio	D. Suichu
1	Grumman Aircraft Engineering Corp. Bethpage, Long Island, New York	Joseph Gavin
1	Kidde Aero-Space Division Walter Kidde and Company, Inc. 675 Main Street Belleville 9, New Jersey	R. J. Hanville Director of Research Engineering
1	Lockheed California Company 10445 Glen Oaks Boulevard Pacoima, California	G. D. Brewer
1	Lockheed Missiles and Space Company Attn: Technical Information Center P. O. Box 504 Sunnyvale, California	Y. C. Lee Power Systems R&D
1	Lockheed Propulsion Company P. O. Box 111 Redlands, California	H. L. Thackwell
1	The Marquardt Corporation 16555 Saticoy Street Box 2013 - South Annex Van Nuys, California	D. L. Walter
1	Martin Division Martin Marietta Corporation Baltimore 3, Maryland	John Calathes (3214)

DISTRIBUTION LIST CONTINUED

COMMERCIAL CONTRACTORS

COPIES	RECIPIENT	DESIGNEE
1	Stanford Research Institute 333 Ravenswood Avenue Menlo Park, California	Thor Smith
1	TAPCO Division Thompson-Ramo-Wooldridge, Inc. 23555 Euclid Avenue Cleveland 17, Ohio	P. T. Angell
1	Thiokol Chemical Corporation Redstone Division Huntsville, Alabama	W. L. Berry
1	United Aircraft Corporation Research Laboratories 400 Main Street East Hartford 8, Connecticut	Erle Martin
1	United Technology Center 587 Methilda Avenue P. O. Box 358 Sunnyvale, California	B. Abelman
1	Vought Astronautics Box 5907 Dallas 22, Texas	Warren C. Trent